Japan Geoscience Union Meeting 2015
(May 24th - 28th at Makuhari, Chiba, Japan)

SVC46-01 Room:304 Time:May 24 16:15-16:30

A petrological test of the earthquake-trigger model of the Mt. Fuji Hoei eruption

ARUGA, Takafumi[1*] ; NAKAMURA, Michihiko[1] ; OKUMURA, Satoshi[1] ; YOSHIMOTO, Mitsuhiro[2]

[1]Department of Earth Science, Graduate School of Science, Tohoku University, [2]Mount Fuji Research Institute, Yamanashi Prefectural Government

It is fairly widely recognized that huge earthquakes may trigger volcanic eruptions. The statisitic validity of this "hypothesis" is, however, under debate. Besides, only little is understood about the triggering mechanisms and resulting incubation period from the earthquake to the eruption. The Hoei eruption of the Fuji volcano in 1707 A.D. occurred 49 days after the Hoei M 8.7 earthquake, and thus often referred as a typical example of the earthquake-triggered eruption. This clear paleographic record of the incubation period provides us an excellent opportunity to test the cause-and-effect link between the huge earthquake and magmatic eruption. Fujii (2002) proposed a triggering mechanism of the Hoei eruption, in which basaltic magma injected into the shallow dacitic magma chamber and induced volatile exsolution. In this study, we elucidate the timescale from magma injection to eruption from the mineralogical record in the Hoei erupted materials, and compare the result with the known interval of 49 days.

We found reverse zonings of plagioclase phenocrysts in the basaltic scoriae. The phenocrysts were considered to have been derived from the dacite magma because their core compositions are consistent with those in the silicic magma initially erupted in the Hoei sequence. Based on the measured MgO concentration profiles, we can estimate the timescale of magma mixing and then test the scenario that the Hoei eruption was triggered by the Hoei earthquake. The temperature of basaltic magma of the Hoei eruption was estimated to be 1080-1180 (Sato & Hara, 1990). With this temperature range, the timescales of magma mixing were calculated to be 45.9, 9.6 and 2.2 days at 1080, 1130 and 1180 ℃, respectively. Because these estimated timescales are shorter than 49 days, the mixing should have started after the Hoei earthquake. On the other hand, the estimated timescales are longer than the duration of the Hoei eruption, showing that the mixing was not syn-eruptive but preeruptive. These results support a model that the Hoei earthquake triggered the injection of basaltic magma into the shallow dacite magma chamber, leading to the Hoei eruption.

Keywords: Fuji Volcano, Hoei Eruption, Hoei Earthquake, Eruption Trigger, Tracer Element Diffusion

SVC46-02 Room:304 Time:May 24 16:30-16:45

Evaluation of elastostatic effects of large earthquakes on the dike system around Mt. Fuji

HOSONO, Masaki[1*] ; MITSUI, Yuta[2] ; ISHIBASHI, Hidemi[2]

[1]Faculty of Science, Shizuoka University, [2]Institute of Geosciences, Shizuoka University

A recent study (Chesley et al., 2012) focused on mechanical effects of earthquakes on volcano systems, and calculated static stress change on the main dike of Mt. Fuji by the 1707 Hoei earthquake and the 1703 Genroku Kanto earthquake. In this study, we first performed validation tests of this previous study using my own codes, and confirmed that my calculation results and their results are the same. And then, we did the similar research calculating the normal stress perpendicular to the main dike and another dike that turned to be active after the 2011 Tohoku-oki earthquake. We examined the static stress changes on both dikes, by not only two earthquakes but nearby large earthquakes (the 762 Mino-Hida-Shinano earthquake, the 2011 Tohoku-oki earthquake, and possible Fujigawa-kako earthquake) as scenario earthquakes. The calculation results showed that the earthquakes having potentials to induce the eruption of Mt. Fuji were the Hoei earthquake and the Tohoku-oki earthquake, and the Fujigawa-kako earthquake. Moreover, we propose that the large earthquakes can be the switches of the dike activities beneath Mt. Fuji.

Keywords: Mt. Fuji, dike, large earthquakes, static stress changes

Japan Geoscience Union Meeting 2015
(May 24th - 28th at Makuhari, Chiba, Japan)

SVC46-03 Room:304 Time:May 24 16:45-17:00

Magma ascent process during the late stage of Fuji 1707 eruption; constraints from plagioclase microlite

AMANO, Yamato[1*] ; ISHIBASHI, Hidemi[1] ; HOKANISHI, Natsumi[2] ; YASUDA, Atsushi[2]

[1]Guraduate School of Science, Shizuoka university, [2]Earthquake Research Institute, University of Tokyo

The Hoei eruption occurred at 1707 is the latest eruption of Fuji volcano. Plinian to sub-plinian eruption continued ca. 15 days with several times of pause during the eruptuin. Plinian and sub-plinian eruption of chemically homogeneous basaltic magma continued after the third days although dacitic-andesitic magma erupted in the early two days. At the end of the eruption, scoria cone was formed in the first crater, indicating transition of eruption style from plinian or sub-plinian to strombolian. However, the cause of this transition is not understood. In this study, textural and chemical analyses are done for plagioclase microlites in scoria samples collected from plinean fall deposit and the last scoria cone of Hoei eruption to clarify conduit ascent process in the late stage and the cause of the transition occurred at the end of the eruption.

Scoria samples of plinian and strombolian eruptions were collected from fall deposit located ca. 8km east from the source and from the scoria cone in the first crater. Among them, 30 scoria grains of the late stage continuous eruption called as Ho-IV stage, 5 grains for each of 6 units, and 4 strombolian scoria samples were investigated in terms of chemical composition, crystal size and crystal number density of plagioclase microlites. Chemical compositions of plagioclase microlites were analysed using EPMA (JEOL-8800R) at Earthquake Research Institute, University of Tokyo. Microlite size and number density were measured by image analyses of BSE images acquired by using SEM at Michibayashi Lab., Shizuoka University.

Both of plinian and strombolian scorias are aphyric with very trace amount of plagioclase and olivine phenocrysts rarely accompanied with pyroxenes. Maximum An number [=100Ca/(Ca+Na)], maximum size and crystal number density of plagioclase microlites are ca. 74.4, ca. 191μm, and ca. 1240 /mm^2 in the plinean scoria and ca. 78.3, ca. 293μm, and ca. 881/mm^2 in the strombolian scoria, respectively; maximum An number and maximum size are larger and crystal number density is lower for plagioclase micrlites in the strombolian scoria than those in plinean scoria.

Based on phase relation, eruption temperature was estimated to be ca. 1135 ℃. The pressure at which crystallization of plagioclase microlite started were estimated by using plagioclase-melt geohygrometer of Putirka (2008) to be ca. 21 MPa for plinian and ca. 24 MPa for strombolian eruptions, corresponding to depths of ca. 840-870m and ca. 940m, respectively. Conduit ascent velocities at the depths of microlite crystallization were estimated from number density of plagioclase microlites by using the MND water exsolution rate meter of Toramaru et al. (2008) to be ca. 54 km/h and 36 km/h for plinean and strombolian eruptions, respectively. The ascent velocity of plinian eruption was 1.5 times faster than that of strombolian eruption. Present results suggest that conduit ascent velocity decreased at the end of Hoei eruption, resulting in plinian-strombolian transition. The ascent velocity decrease was caused by phenomena occurred at depth $>$940m, such as decrease in conduit width and/or overpressure in magma reservoir.

Keywords: Fuji volcano, plagioclase, microlite, conduit ascent velocity, scoria, eruption style

SVC46-04 Room:304 Time:May 24 17:00-17:15

Recycling of pyroclasts controls style of small basaltic explosion at Stromboli Volcano, Italy

MIWA, Takahiro[1*] ; KAWAGUCHI, Ryohei[1] ; NISHIMURA, Takeshi[2] ; AOYAMA, Hiroshi[3] ; YAMADA, Taishi[3] ; FUJITA, Eisuke[1]

[1]NIED, [2]Tohoku Univ, [3]Hokkaido Univ

Understandings of controlling mechanism on eruptive style is one of the most important subject not only for volcanology but also for hazard mitigation. Vesiculation, outgassing and crystallization that drive or break their ascent have been considered as essential factors for the controlling mechanism (e.g., Jaupart and Allegre, 1990; Houghton and Gonnerman, 2005). In contrast, recent studies have suggested that vigorous recycling of pyroclast into the vent occurs at basaltic volcano where small explosions are repeated (D'Oriano et al., 2014; Eychenne et al., 2014). The recycling of pyroclast that fills the vent can affect explosion dynamics such as shape and ejection speed of jet cloud (Goto et al., 2001; Ohba et al., 2002; Taddeucci et al., 2013).

This study examined component, texture, granulometry and chemical composition of ash samples from normal activity at Stromboli to discuss a controlling mechanism of explosion style of small basaltic explosion. Stromboli volcano has three vent regions as northeast (NE), central (C), and southwest (SW) craters. The three craters emitted white steam continuously that was interrupted by relatively strong explosion. During studied term (14:26-18:29, May 21th, 2014), different explosion styles were observed in each vents. The NE crater exhibited explosive emission of ash rich cloud, and the C and SW craters showed emission of glowing bomb with dilute ash cloud. We collected falling ash from the three craters every 4-18 minutes. Although the samples contain ash particles from the three craters, ash falling rate at sampling site becomes large after occurrence of ash rich explosion at NE crater. The ash particles are divided into Juvenile (glassy particle with elongate, spongy, or dense morphology), Recycled (non-glassy particles with highly crystalline which has similar texture with product of reheating experiment of basaltic ash; D'Oriano et al., 2013), Altered, and Crystal particles. The origin of the each type of particles are interpreted on the basis of their external and internal textures observed under stereoscopic and electron microscope (D'Oriano et al., 2014). We calculated bulk componentry using the componentry variations with grain size (125-250, 250-500, 500-1000, and 1000-2000μm) and grain size distribution. The bulk componentry shows that the volume fraction of recycled particles increases with ash falling rate at sampling site that concords the occurrence of ash rich explosion at NE crater.

The ash observation implies that burial of eruptive vent by recycled particles relates with occurrence of ash rich explosion at NE crater. The explosion occurs at which the gas rich magma from deeper conduit (e.g., Ripepe et al., 2001; Lautze and Houghton, 2007) reaches to the boundary between magma column and buried sediment. Emission of gas jet by the explosion blows the sediment which buries the vent-conduit (Patrick et al., 2007). Thick sediment can store large amounts of gas, magma and heat that generate ash rich cloud at the blowing. Therefore, we suggest that thickness of buried sediment is one of a controlling factor for the style of small basaltic explosion.

Keywords: eruptive style, recycling, basaltic magma, volcanic ash, Stromboli volcano

Japan Geoscience Union Meeting 2015
(May 24th - 28th at Makuhari, Chiba, Japan)

SVC46-05 Room:304 Time:May 24 17:15-17:30

Spatio-temporal changes of magma pressure in the conduit at Stromboli as inferred from analyses of tilt records

KAWAGUCHI, Ryohei[1*] ; NISHIMURA, Takeshi[2] ; AOYAMA, Hiroshi[3] ; YAMADA, Taishi[3] ; MIWA, Takahiro[1] ; FUJITA, Eisuke[1] ; GENCO, Riccardo[4] ; LACANNA, Giorgio[4] ; RIPEPE, Maurizio[4]

[1]NIED, [2]Science, Tohoku Univ., [3]Science, Hokkaido Univ., [4]Firenze Univ.

Recent geodetic observations at active volcanoes succeeded in detecting volcano deformations prior to a small volcanic explosion. These could be used for quantitatively understanding the magma ascent processes before eruptions. We installed three tilt meters and one broadband seismometer within a distance of 500 m from the active craters at Stromboli volcano, Italy, in the end of May 2014, and recorded large number of tilt data associated with explosions until September. In this study, we estimate the spatio-temporal changes of magma pressure in the conduit by using these tilt data.

We analyze tilts of 26 events recorded with high S/N ratio. These tilts at the three stations show uplifts toward craters from about 200 s before each explosion that is detected as an onset of seismic signal. By examining tilt vectors, we found that the tilt vectors roughly point to the direction of NE crater, and the direction of tilt vectors rotate about 5 seconds before the start of seismic signal. These characteristics are observed in the 22 events among 26 explosions.

To estimate the location of the source of tilt motions, we calculate the tilt motions due to pressure changes in an open conduit located at NE crater taking into account the topography of Stromboli volcano. The calculation results show that the directions of tilt vectors are changed by the difference in the depth of pressure source. We interpret that from few minutes to 5 seconds before an eruption magma pressure increases at the depth of about 50-100m below the crater. Then just before the eruption, the pressure source becomes deeper, down to about 150 m below the crater.

Keywords: Tilt motion, Strombolian eruption, Pressure source

Japan Geoscience Union Meeting 2015
(May 24th - 28th at Makuhari, Chiba, Japan)

SVC46-06 Room:304 Time:May 24 17:30-17:45

Plinian eruptions without precursory basalt injection: Case study of the Sakurajima historic eruptions

ARAYA, Naoki[1*] ; NAKAMURA, Michihiko[1] ; OKUMURA, Satoshi[1]

[1]Department of Earth Science, Graduate School of Science, Tohoku University

Injection of new magma into a shallow differentiated magma chamber is often considered as a trigger of volcanic eruptions. This is primary based on the petrological observation that magma mixing precedes the eruptions by a short interval. However, some petrological records such as oscillatory zoning of phenocrysts, in addition to geophysical monitoring of active volcanoes (e.g. Iguchi et al., 2008), suggest that magma injections had occurred repeatedly without triggering eruptions immediately. In such a case, the mafic magma injection may be regarded as a preparation process for eruption rather than a trigger. To clarify the magma injection and accumulation processes prior to the past large eruptions is crucial for forecasting the volcanic activity. For this purpose, we investigated the pumice clasts of the three historic Plinian eruptions of the Sakurajima volcano, Kyusyu Japan in 1914-1915 (Taisho Era), 1779-1780 (Anei) and 1471-1476 (Bunmei). We have focused on compositional zoning of magnetite phenocrysts, because element diffusion in magnetite is relatively fast and thus has high time resolution.

The magnetite phenocrysts showed scarce compositional zoning in all the eruptions. This result indicates that the last magma injections occurred more than a few months before the eruptions. Hence, we infer that the magma injection did not trigger the historic eruptions immediately. This leads to an implication that a Plinian eruption may occur in the Sakurajima volcano without the injection of new magma prior to several months.

Keywords: Sakurajima Volcano, eruption trigger, magnetite, magma injection, magma mixing

Japan Geoscience Union Meeting 2015
(May 24th - 28th at Makuhari, Chiba, Japan)

SVC46-07 Room:304 Time:May 24 17:45-18:00

Estimation of surface tension of lava from lava stalactite and lava stalagmite appeared in lava tube cave and tree mold

HONDA, Tsutomu[1]*

[1]NPO Vulcano-Speleological Society

[Introduction] Inside the lava cave and lava tree mold void formed by the basalt lava flow, lava stalactite and lava stalagmite are often observed. It is a phenomenon which the droplet of lava falls from a ceiling and deposits on the floor. The estimation of surface tension of lava from the pitch of lava stalactite and size of lava stalagmite appeared in lava tube cave and tree mold void are performed and compared with various lavas.

[Estimate of surface tension from lava stalactite] Lava stalactites are positioned periodically on the surface of the ceiling wall or side wall. From the periodical pitch of the stalactites, we can obtain the surface tension of the lava. The pitch will be critical wave length of the occurrence of instability of thin liquid film attached on the surface of the ceiling of the lava tube cave or lava tree mold void. The pitch P is shown as P=$2\pi(\gamma/g\rho_L)^{1/2}$, where$\gamma$is surface tension of liquid ρ_L is density of liquid, g is gravity acceleration. From the pitch of lava stalactites on the roof surface (P=3 to 4cm), the surface tension of lava γ=$P^2g\rho_L/4\pi^2$ was determined as 560~990 dyne/cm.

[Estimate of surface tension from lava stalagmite] After the droplet's falling either from the liquid layer of a ceiling or from a straw formed from a ceiling, the droplets of lava may be acumulated one after another on the floor. The cylindrical configuration of the lava droplet has a certain radius and length in such a way that the configuration of the droplets has almost the same size. It is thought that the surface tension of the droplet is playing an important role in this phenomenon. When it becomes impossible for surface tension to bear the weight of the droplet, the droplet will fall down. After that, again the liquid lava will be supplied, then, the droplet will repeat to fall down. Consequently many lava droplets will be deposited on a floor area. This phenomenon is very similar to the "weight of falling drops technique" which is the general method of measuring the surface tension of a liquid. Based on this idea, the study model for determining the surface tension $\gamma$of lava is made. When mass of the droplet is set to m, the force which pulls the droplet downward is f_1=mg (g is acceleration due to gravity), and the force of pulling up this upwards is $f_2=2\pi r\gamma$, where r is the radius of the lava droplet. The surface tension $\gamma$is calculable for $f_1=f_2$if the weight of the lava droplet is known. As $f_1=mg=\pi r^2 l\rho_L g$, where l is length of the lava droplet, ρ_L is the density of the lava, the surface tension $\gamma=rl\rho_L g/2$ can be obtained from r and l of the lava droplets accumulated on the floor. If we introduce ρ_L=2.5g/cm^3 and g= 980 cm/s^2, and by the fields observation of r and l, for example, the surface tension γ=490 dyne/cm can be obtained for r=0.2 cm, and l=2cm, and γ=980 dyne/cm can be obtained for r=0.25 cm, and l=4cm.

[Conclusions] The value of such surface tension obtained from the lava stalagmite is in good agreement with the surface tension acquired from the pitch of the waving of the liquid layer by the simple hydrodynamic instability model of gravity/surface tension acting on the melting liquid layer attached on the inner surface of the lava cave. This value also agrees well with the extrapolated value obtained by I. Yokoyama and S.Iizuka[1)] in the melting lava surface tension measurement experiments in Laboratory. As a conclusion, we could say that the surface tension plays a preponderant role for the lava stalactite and stalagmite formation in the lava cave and lava tree void. It seems that there is no significant difference between surface tensions of different basaltic lavas though further study for various lavas will be continued .

[References]

1) I.Yokoyama,S.Iizuka(1970):Technical Report,Hokkaido Univ. p57

Keywords: lava tube, volcanic cave, surface tension, lava tree mold

SVC46-07 Room:304 Time:May 24 17:45-18:00

Name of Volcano, Area	SiO_2 weight%(Reference), Eruption year	Cave or T-Mold	Measured P , r and ℓ	Estimated surface tension
Mt Fuji,Inusuzumi-yama, Mitsuike-ana	49.09%(H.Tsuya) , before 7000	Cave	P=3～4cm r=0.2~0.25cm,ℓ=2~4cm	560～990dyne/cm 490～980 dyne/cm
Izu-Osima, Mihara-yama	52~53%(T.Minakami), 1951	Cave	P= ～3cm	～560 dyne/cm
Shimane,Daikon-zima	47%(I.Sawa), before 190000	Cave	P= ～3cm	～560 dyne/cm
France, Reunion, Le Piton de la Fournaise	48.8~49.8% (N.Villeneuve),1998 48~50% (A.Peltier),2004	Cave	P=3～4cm r=0.2~0.25cm,ℓ=2~4cm	560～990 dyne/cm 490～980 dyne/cm
Vietnam, Central Plateau, Chupluk Volcano	48~52% (N.Hoang)	Cave	P=3～4cm	560～990 dyne/cm
Mt Fuji,Ken-marubi, Funatsu-tainai	50.88%(H.Tsuya), 937	T-Mold	P=3～4cm	560～990 dyne/cm
Mt Fuji,Ken-marubi, Yoshida-tainai	50.88%(H.Tsuya), 937	T-Mold	P=3～4cm	560～990 dyne/cm
Izu-Osima, Mihara-yama	52%(S.Nakano, T.Yamamoto), 1986	T-Mold	P=～4cm	～990 dyne/cm
Miyake-zima, O-yama	53~54%(T.Fujii et al),1983	T-Mold	r=0.1~0.25cm, ℓ=5cm	610～1530 dyne/cm
Hachijo-zima,Nishi-yama,	50.4~50.5%(M.Tsukui), Before 1100	T-Mold	P=3～4cm, r=0.2~0.25cm,ℓ=2~4cm	560～990 dyne/cm 490～980 dyne/cm
US,Oregon,Newberry Volcano, Lava cast forest	49～50%(J.Donnelly), Before 7000	T-Mold	P=3～5cm	560～1740 dyne/cm

Japan Geoscience Union Meeting 2015
(May 24th - 28th at Makuhari, Chiba, Japan)

SVC46-08 Room:304 Time:May 25 09:00-09:15

Plinian eruption preceded by disruption of lava dome at Kelud volcano, Indonesia, in 2014

MAENO, Fukashi[1*] ; NAKADA, Setsuya[1] ; YOSHIMOTO, Mitsuhiro[2] ; SHIMANO, Taketo[3] ; HOKANISHI, Natsumi[1] ; AKHMAD, Zaennudin[4] ; IGUCHI, Masato[5]

[1]Earthquake Research Institute, University of Tokyo, [2]Mount Fuji Research Institute, Yamanashi Prefectural Government, [3]Graduate School of Environment and Disaster Research, Tokoha University, [4]Center for Volcanology and Geological Hazard Mitigation, Indonesia, [5]Sakurajima Volcano Research Center, Disaster Prevention Research Institute, Kyoto University

Kelud volcano, Indonesia, is an active andesitic stratovolcano that has repeatedly erupted over many centuries. After a quiescent period since the dome-building eruption in 2007-2008, a plinian eruption with a radially spreading umbrella cloud at 18 km height occurred in February 2014. We present results of field observations, and discuss the sequence of this plinian event, with estimation of some physical parameters controlling eruption dynamics.

Eruptive deposits can be divided into three major units, Unit A to C, which corresponds to the main stages of this event. Unit A is pyroclastic density current deposits characterized by massive, poor-sorted, and composed of pumice, lithics and woods fragments. The distribution is limited to the northeastern side of the volcano, and extends up to ˜5 km from the summit. In distal area, this unit consists of a thin fine ash layer. Numerous trees blown down on the substrate in the northeast also belongs to the same unit. Unit B is pyroclastic fallout deposits. In proximal area, the unit is characterized by thick fallout deposits containing large pumice clasts and lava blocks. This unit underlies numerous ballistic ejecta originating from andesitic lava dome produced in 2007-2008. In distal area, the same unit is recognized as a thin ashfall layer. This unit is widely distributed from north to southwest. At Jogjakarta ˜200 km away, ˜2 cm ashfall was observed. This observation is consistent with satellite data showing the plinian plume drifted by strong easterly wind and dispersed mainly western side of the volcano. Unit C is poor-sorted, pumice-rich pyroclastic density current deposits that are distributed along southern and western valleys up to 3-4 km. Multiple, pumice-rich flow lobes are well developed. Large pumice clasts are generally concentrated in the upper part and flow front of the deposits. In the northern side, this unit is recognized as normally graded, fine ashfall layers. After the eruption, a number of secondary phreatic explosions occurred from the valley-filled pumice-rich deposits, and created explosion craters.

Volume of tephra fallout from all stages is estimated to be 0.32-0.46 km^3, using relationships between dispersal area and tephra thickness. A total volume of pyroclastic density current deposits for Stages 1 and 3 was estimated to be ˜0.1 km^3 based on the deposit distribution and thickness assumption. Duration of plume development was estimated to be 2.5-3 hours based on satellite images. From the tephra volume and eruption duration, mass discharge rate was calculated to be in the range 5.6?8.6$*10^7$ kg/s.

Our field observation suggests that, in Stage 1, pyroclastic density currents run at least 5 km to the northeastern side with blowing off vegetation including numerous trees. Perhaps, the 2007-2008 lava dome acted as a cap-rock of conduit, and it was partially destroyed from the northern edge. Initially, the eruption couldn't produce a buoyant steady column from an open conduit, but generated energetic and directed pyroclastic density currents (like a blast) from the partially disrupted dome. Then, the dome was completely destroyed and blown away by ascending magma, and the eruption entered the stable plinian phase, Stage 2. Within 3 hours, magma discharge rate decreased, and column collapse began. The eruption stage moved to Stage 3, when pumice-rich pyroclastic density currents occurred. They could run along valleys and buried them with multiple pumiceous flow lobes.

The plinian eruption in 2014 was characterized by a strong eruption plume preceded by blowing off lava dome and generation of energetic pyroclastic density currents. Also other pyroclastic density currents by column collapse followed the plinian eruption. Deposit data suggests that the scale of eruption is ranked as VEI 4 and one of the largest eruptions at Kelud volcano in the last few centuries.

Keywords: Kelud, Plinian, Lava dome, Pyroclastic density currents

SVC46-09 Room:304 Time:May 25 09:15-09:30

Pyrrhotite oxidation as an indicator of air entrainment into eruption columns and lava flows

MATSUMOTO, Keiko[1*] ; NAKAMURA, Michihiko[1]

[1]Department of Earth Science, Graduate School of Science, TOHOKU University

Air entrainment into eruption columns plays an important role for volcanic eruption dynamics as it causes buoyancy and temperature decrease for erupted materials. In this study, we develop a new method for quantifying the degree of air entrainment on the basis of Pyrrhotite (Po) oxidation reaction.

Since fO_2 of air is ca. 10 log units higher than that of the typical arc pre-eruptive magmas, oxidation of magmas may sensitively reflect the air entrainment. The oxidation reaction of Po proceeds quickly at high temperature within a several tens of seconds to a several tens of hours. Because this timescale corresponds to the typical eruption duration, the reaction may record the eruption dynamics. Matsumoto and Nakamura (2012) found Po crystals and their oxidized texture in the Sakurajima 1914-15 (Taisho) Plinian pumice clasts. In this study, we have additionally examined clastogenic lava (CL) (Yasui et al., 2007) and effusive lava (EL) samples of the Taisho eruption and estimated the Po oxidation conditions.

The oxidation products were identified as magnetite (Mt) and hematite (Hm) with reflective microscope and Raman spectroscopy. The Mt and Hm crystals were found to be Ti-free by using X-ray mapping except for the phenocrysts in the EL samples. The representative occurrence of Po and its oxidation texture were summarized as follows: In the pumice samples, unreacted Po was observed as well as relict Po with Mt-Hm composite reaction rims. In the CL, unreacted Po grains scarcely found and almost all the oxidation products were Hm. In the EL sample, unreacted Po, relict Po with Mt rim, Po pseudomorphs replaced entirely by Mt and Hm, and those by Hm existed. In contrast to the pumice clasts, no three-phase coexistence in a grain was found.

This occurrence of Po and oxides can be explained in terms of the 'achieved fO_2' and 'high-T and high- fO_2 duration'. The 'achieved fO_2' will be scaled by (A) pre-eruptive magma: $10^{-7.5}$?$10^{-9.0}$ bar, (B) equilibrium of Po and Mt: $10^{-6.9}$?$10^{-8.3}$ bar, (C) equilibrium of Mt and Hm: $10^{-4.7}$?$10^{-6.2}$ bar according to Matsumoto and Nakamura (2012), Huebner and Sato (1970) and Eugster and Wones (1962), and (D) the partial pressure of O_2 in air: $10^{-0.7}$ bar. Time scales of 'high-T and high- fO_2 duration' can be calculated by using (i) reaction duration for Mt rim of Po, (ii) reaction duration for Hm rim of Mt, and (iii) Ti diffusion time in Mt. Using these scales, occurrences of oxidation textures in each sample can be explained as follows: In the Plinian pumices, about half of the grains were not accompanied by oxides rim, showing that their achieved fO_2 were below (B); the rest of the grains having Hm rims experienced the fO_2 above (C). The grains between (B) and (C) rarely existed. The reaction duration of the pumices were estimated to be $<$3.5 hours (iii). The variation in the degree of oxidation reaction in the pumices can be interpreted to reflect the variation in the degree of contact with air and cooling process. The oxidation reaction of Po in CL occurred at fO_2 above (C) and was ceased in 6.3 to 22 hours (ii). The high fO_2 and relatively long reaction duration of CL is consistent with its origin; the CL magma was once fragmented, reacted with air and then welded and kept at high temperature. In EL, about half of the grains were unreacted at fO_2 below (B) and the rest grains were oxidized at fO_2 of (B) to (D). The estimated reaction duration for EL was 3.6 to 33 hours (iii). This fO_2 variation may be caused by partial fragmentation and welding with open system degassing or mixing with oxidized lava crusts. The systematic correlation between the Po oxidation reaction and the eruption processes suggests a possibility that Po oxidation can be an indicator of air entrainment into eruption columns and lava flows.

Keywords: oxidation, air entrainment, pyrrhotite, fO_2, Sakurajima

Japan Geoscience Union Meeting 2015
(May 24th - 28th at Makuhari, Chiba, Japan)

SVC46-10 Room:304 Time:May 25 09:30-09:45

Model of phreatic eruptions inferred from the 2014 eruption of Ontake Volcano

IDA, Yoshiaki[1*]

[1] Advance Soft Co.

A phreatic eruption (phreatic explosion) happened at Ontake Volcano on September 27, 2014 accompanied by more than 50 casualties including mountain climbers who were caught by volcanic smokes or hit by volcanic bombs. Phreatic eruptions often occur in many active volcanoes but what causes them is less understood compared with magmatic eruptions for some reasons as smaller scales and less influence to people. For that phreatic eruption of Ontake Volcano video images and deformation data that revealed basic natures of the eruption were obtained. Based on these data the present paper proposes a model that may be useful for a better understanding and simulation of eruptive processes.

A video camera at Takigoe Observation Point, Ministry of Land gave an interesting image about initial features of the Ontake eruption that began about 11: 55 a.m. even if the eruption point itself was obscured by clouds. In the summit area with weak fumaroles the eruption suddenly emitted voluminous dark gas, which first flowed down about 3 km long as a pyroclastic flow and then ascended as a plume. The plume reached the height up to 8 km above the sea level according to a radar measurement. Another video image taken from a helicopter about 2:00 p.m. showed that the plume was substantially weakened and split into several separate gas flows.

The gas that was emitted at an early stage of the eruption was very dark and moved down as a pyroclastic flow so that it should have contained abundant solid particles with a higher density than the air. Rich solid particles in the gas explain lots of volcanic bombs and thick ash deposits actually observed near the summit. The gas flow is understood to have turned to a plume when it deposited part of solid particles. It is likely that solid particles were generated by erosion of the permeable layer through which steam migrated to the surface and that resultant high permeability allowed the steam to flow violently out during the eruption.

The tilt data obtained at Tanohara Observation Point, Japan Meteorological Agency gives another important constraint on the eruption process. The data revealed that inflation first took place below the eruption point during about 7 minutes and then contraction followed as soon as the eruption started.

The inflation prior to the eruption was likely caused by increase of vapor in the underground water system. Simple vaporization, however, cannot produce inflation because successive vaporization is suppressed by pressure increase. Inflation often arises in volcanoes when some material ascends under gravity. Here, the process in which steam bubbles generated at the bottom ascend through the ground water is considered. The bubble formation may result from a thermal instability due to heat supply to the bottom consistently with no significant seismicity observed with the inflation.

The above idea gives a model of phreatic eruptions in the system of steam overlying ground water. The equilibrium described by an evaporation curve is assumed to hold at the interface between steam and water. The steam flux generated at the bottom of the ground water is prescribed as a function of time. The steam is assumed to migrate to the surface as a permeable flow and the effect of erosion is represented by the change of permeability whose speed is defined by a prescribed function of steam flux and permeability.

In this model pressure, permeability and gas fluxes are calculated as a function of time from a set of ordinary differential equations derived from conservation laws and thermodynamic relations. The differential equations give the solutions that qualitatively reproduce pre-eruptive underground inflation followed by rapid gas effusion during the eruption if constants and initial values of variables are suitably prescribed..

Keywords: phreatic eruption, phreatic explosion, Ontake Volcano, pyroclastic flow, crustal deformation, computer simulation

SVC46-11 Room:304 Time:May 25 09:45-10:00

A numerical study of pyroclastic flow dynamics: Development of a two-layer model based on Shallow-Water equations

SHIMIZU, Hiroyuki[1*] ; KOYAGUCHI, Takehiro[1] ; SUZUKI, Yujiro[1]

[1]Earthquake Research Institute, The University of Tokyo

Pyroclastic flows are density currents of mixtures of volcanic particles and gas that flow on the ground surface. They are characterized by wide ranges of density ratio $\rho/\rho_a(\sim 10^0\text{-}10^3)$, where ρ and ρ_a are the densities of current and ambient, respectively. The dynamics of pyroclastic flows are affected by many physical factors such as settling of particles and entrainment of ambient air. In order to understand these effects on the dynamics of pyroclastic flows with wide ranges of ρ/ρ_a, we have developed a new numerical model based on shallow-water equations. The model has been verified by applying it to the dam-break problem, for which analytical solutions of different fluid dynamical stages are available.

In order to calculate the dynamics of pyroclastic flows with wide ranges of ρ/ρ_a using the shallow-water equations, the balance between the driving force and the dynamic reaction at the flow front (i.e., front condition) should be correctly taken into account. In previous works, two types of numerical models have been proposed to express the front condition: Boundary-Condition (BC) type model and Artificial-Bed (AB) type model. BC type model is a numerical method in which the front condition is applied to the boundary condition at the flow front. In AB type model, the front condition is calculated by setting a thin artificial bed ahead of the front. We have revealed that AB type model is applicable to the currents of $\rho/\rho_a \geq 100$, whereas BC type model should be used for the currents of $\rho/\rho_a \leq 100$. We have also developed a rigorous algorithm calculating the front condition using BC type model.

Our numerical method enables us to investigate the effects of the settling of particles and the entrainment of ambient air on the flow dynamics for wide ranges of ρ/ρ_a. Particle settling decelerates the front speed and enhances the formation of "jump" that separates the current into head and tail parts. Entrainment of ambient air also decelerates the front speed and suppresses the formation of the jump between the head and the tail of the current. Our results also suggested that the rate of entrainment tends to increase as ρ/ρ_a increases. When both the effects of particle settling and entrainment are present, the competition between these two effects is considered to result in diverse flow patterns.

Pyroclastic flows with large density gradients are generally divided into a dilute overriding part ($10^0 \leq \rho/\rho_a \leq 10^1$) and a dense basal part ($\rho/\rho_a \sim 10^3$). In order to simulate the dynamics of such realistic pyroclastic flows, we have developed a two-layer model where the dynamics of the dilute overriding part is solved by BC type model and that of the dense basal part is solved by AB type model. In the dilute overriding part, the effects of the settling of particles and the entrainment of ambient air are taken into account. In the dense basal part, the effects of the settling of particles and the basal friction are taken into account. We present some preliminary results showing temporal evolutions of the dilute overriding part, the dense basal part and the deposits.

Keywords: pyroclastic flows, density currents, gravity currents, Shallow-Water equations, two-layer model

SVC46-12 Room:304 Time:May 25 10:00-10:15

Effects of vertical diffusivity and plume shape on the inversion analysis of tephra fallout deposits

KIYOSUGI, Koji[1*] ; KOYAGUCHI, Takehiro[1] ; SUZUKI, Yujiro[1]

[1]Earthquake Research Institute,The University of Tokyo

Estimation of volcanic plume condition from fallout deposits is an important volcanological subject; such estimations are indispensable for reconstruction of the dynamics of volcanic plumes in the past as well as forecast of tephra fallout distribution during ongoing eruptions. The goal of this study is to develop an accurate inversion method to estimate tephra source parameters (location, height, amount and grain size of tephra) from distribution of tephra fallout deposits. In previous studies on the inversion analyses using tephra fall deposits (e.g., Klawonn et al., 2012; Mannen 2014), vertical diffusivity of particles and bending of volcanic plume due to wind are sometimes assumed to be negligible. In this study, we investigated the applicability of these assumptions through systematic advection-diffusion simulations of single-sized tephra particles released from point sources above a vent.

In the advection-diffusion simulation of single-sized particles from a point source, the released particles diffuse and form a ”particle cloud”. If the vertical diffusivity of particles is ignored, particle clouds diffuse only horizontally and the distribution of particles is described by a bivariate Gaussian distribution (BGD). On the other hand, when the vertical diffusion exists, the particle cloud has an oblate spheroid shape. Because of the presence of wind, the vertically extending particle cloud keeps its horizontal movement after the landing of its bottom until the settlement of its top. As a result, the distribution of deposits deviates from a BGD in three ways: (1) increase of the kurtosis in the cross wind direction, (2) increase of the skewness and (3) increase of the variance along the wind direction. Among these deviations, (1) and (2) are caused by vertical diffusion of particles during deposition of the particle cloud and become significant when $(D_z/v_t z)^{1/2} \geq 0.2$ where D_z is the vertical diffusion coefficient, v_t is the terminal velocity, z is the source height. The deviation (3) is caused by horizontal movement of the particle cloud in the wind direction during the deposition and becomes significant when ${D_z}^{1/2} {D_h}^{-1/2} W {v_t}^{-1} \geq 3$ where W is the wind velocity, D_h is the horizontal diffusion coefficient.

Volcanic plumes generally bent to leeward when wind is present. The effect of bending plumes on the distribution of tephra fallout deposits is evaluated through comparison between the bending distance of the plumes and the advection distance of settling particles. Dimension analysis and wind-affected volcanic plume models (e.g., BENT; Bursik 2001) suggest that the trajectory (bending distance x and height z) of a bending weak plume is approximated by $z=CB^{1/3}W^{-1}x^{2/3}$ (Wright 1971), where C is a constant, B is the effective buoyancy flux (Sparks et al., 1997). On the other hand, the advection distance of particles can be calculated as $b=zW/v_t$. If the bending distance x is as large as the particle advection distance b (i.e., $x/b \geq n$; n is a constant of order 10^{-1}), the effect of bending plumes cannot be ignored; on the basis of the equations of bending distance and advection distance, this condition can be rewritten as $C^{-3}B^{-1}zW{v_t}^2 \geq n^2$.

The above results show that the effect of vertical diffusivity is significant when finer particles are released from lower altitudes. In contrast, the effect of bending plume is significant when coarser particles are released from higher altitudes. The results also suggest that both the effects can be insignificant for particles with intermediate grain size. From the above equations, it is inferred that the terminal velocity of such particles with intermediate grain size ranges $D_z/0.04z \leq v_t \leq nC^{3/2}B^{1/2}z^{-1/2}W^{-1/2}$ when $Wz(D_z D_h)^{-1/2} < 75$ and $W{D_z}^{1/2}/3{D_h}^{1/2} \leq v_t \leq nC^{3/2}B^{1/2}z^{-1/2}W^{-1/2}$ when $Wz(D_z D_h)^{-1/2} > 75$. These relationships between grain size and particle distribution must be taken into consideration in the inversion analysis.

Keywords: volcanic plume, tephra fallout deposits, advection-diffusion model, inversion analysis

SVC46-13 Room:304 Time:May 25 10:15-10:30

A trial of measurement for shape and velocity of ash-fall by using a digital image analysis technique

HATTORI, Yasuo[1*] ; NAKAO, Keisuke[1] ; SUTO, Hitoshi[1]

[1]Central Research Institute of Electric Power Industry

Accurate descriptions of terminal velocity of ash-fall are practical interest in volcanic ash risk assessment on critical infrastructure (e.g. Wardman et al. 2012). Numerical simulations with an ash transport- and deposition-model, which has a capability to estimate spatial- and temporal-distributions of ash concentration and deposition, have become a powerful tool of the risk assessment (e.g. Folch 2012). Such simulations give the solution of governing equations on ash transport processes with numerical procedures. The governing equations include some empirical formulas with assumptions. Also for the estimation of terminal velocity of ash-fall, many empirical formulas have been already reported, but there exists considerable scattering of calculations among them (e.g Folch 2012).

In the present study, we examined a measurement for shape and velocity of ash-fall by employing a digital image analysis technique. We configured the experimental setup based on a shadowgraph particle measurement system of Dantec Dynamics to deal with non-spherical particles. The particles were illuminated by high-intensity pulsed lasers, Nd: YAG laser, with an optical diffuser. A CCD camera was placed in front of the light source, and the camera was equipped with a long-distance microscope lens to obtain visualized images of small particles. We carried out a trial measurement for sedimentation of corrected ash and discussed the optimization of measurement parameters and relationship between shape and velocity of ash-fall in a laboratory test. More details will be presented in the presentation, and we believe that our study must be helpful to develop the numerical simulations for evaluation of volcanic ash risk.

The authors wish to express our gratitude to Mr. Y. Futawatari of Dantec Dynamics, Ltd., Mr. T. Sato and Mr. K. Ota for helpful comments on the design of the optical setup, and to Mr. K. Toshida, Dr. D. Miura and Dr. S. Takeuchi for fruitful discussions on this study.

Keywords: Terminal fall velocity, Particle image velocimetry, Laboratory test, Ash transport- and deposition-model

Japan Geoscience Union Meeting 2015
(May 24th - 28th at Makuhari, Chiba, Japan)

SVC46-14 Room:304 Time:May 25 11:00-11:25

Stokes–DEM coupled simulation for a granular media of magma chamber

FURUICHI, Mikito[1*] ; NISHIURA, Daisuke[1]

[1]Department of Mathematical Science and Advanced Technology, Japan Agency for Marine-Earth Science an

The dynamics of a granular media has been suggested to play an important role in a reheated magma chamber by a hot intrusion (e.g. Burgisser and Bergantz, 2011). Although several mechanisms, such as Rayleigh Taylor instability, unzipping, and rhythmic convection (e.g. Shibano et.al. 2012, 2013) have been proposed for characterizing an evolution of crystalline magma chamber, their contributions in the long geodynamical time scale are not clear yet. Thus we performed dynamical numerical simulations of the granular material in three dimensions to investigate the thermal evolution of the magma chamber.

In order to solve high-viscosity fluid and particle dynamics for modelling a melt–crystal jammed state of the magma, we have developed a coupled Stokes–DEM simulation code with two key techniques: formulation of particle motion without inertia and semi-implicit treatment of particle motion in the fluid equation (Furuichi and Nishiura, G-cubed, 2014). Our simulation can successfully handle sinking particles in a high-viscosity fluid.

In our simulation, the top fluid–particle jammed layer is heated by the hot basal fluid at the bottom. This initial setting represents the first-stage toy model for an erosion process at a melting roof of the magma chamber. We have investigated the dynamical patterns of the settling particles which strongly depend on the rheology of the granular layer. In addition, we have also examined the dynamical role of the density of the basal hot melt. Our numerical result indicates the possibility of the spontaneous formulation of crystal rich layer on the basal dense melt layer.

Keywords: Magma chamber, Viscous granular material, Magmatic dyamics, Reactivation, Discrete element method, Stokes flow

SVC46-15 Room:304 Time:May 25 11:25-11:50

Forecasting the transition of explosive volcanic eruptions using a combined model for conduit flow and eruption column

KOYAGUCHI, Takehiro[1*] ; SUZUKI, Yujiro[1]

[1]Earthquake Research Institute, The University of Tokyo

We have developed a combined model for one-dimensional (1D) conduit flow and three-dimensional (3D) eruption column dynamics in order to forecast the transition of explosive volcanic eruptions.

During explosive eruptions, the ascending velocity of magma typically reaches the sound velocity of the gas-pyroclast mixture at the crater base. In this case, the motion of magma from the magma chamber to the eruption cloud is divided into the following three regions: conduit flow from the magma chamber to the crater base (Region 1), decompression and compression processes inside the crater (Region 2), and eruption column dynamics in the atmosphere (Region 3). According to the approximate solution of the 1D conduit flow model (Koyaguchi, 2005), the flow rate in Region 1 depends mainly on magma-chamber pressure, magmatic properties (e.g., temperature, water content and viscosity), conduit radius and conduit length from the magma chamber to the crater base. The decompression/compression process in Region 2 is essentially controlled by crater geometry; when the depth of crater and the ratio of the cross-sectional areas at the top and the base of the crater are given, exit pressure and exit velocity at the crater top are estimated as a function of flow rate (Koyaguchi et al., 2010). When the exit pressure differs from the atmospheric pressure just above the crater, the fluid dynamical features of the eruption column (i.e., Region 3) are significantly affected by the decompression and/or compression processes just above the crater; the ejected material accelerates or decelerates owing to decompression or compression into the atmosphere. According to 1D steady eruption column dynamics models (e.g., Woods, 1988), the column dynamics after the pressure of the eruption column balances the atmospheric pressure depends on magmatic properties, magma discharge rate, and ascent velocity at the time when the pressure of the eruption column balances the atmospheric pressure just above the crater top. The above consideration suggests that the evolution of conduit-crater geometry as well as that of chamber pressure plays a key role in the transition of explosive eruptions.

In this study, in order to evaluate the effects of conduit-crater geometry on the transition of explosive eruptions, we have derived an approximate solution to calculate the velocity and pressure at the crater top as a function of parameters on crater geometry, and systematically investigate the effects of over- and under-pressure at the crater top on the column dynamics using a 3D column dynamics model (Suzuki et al., 2005). The overall features of column dynamics such as column collapse condition in the 3D simulations are qualitatively consistent with the results based on the combination of the 1D column dynamics model and the 1D decompression/compression model (e.g., Woods and Bower, 1995; Koyaguchi et al., 2010). The 3D simulation results also show some distinct features that cannot be expressed in the 1D models; the over- or under-pressured jets are characterized by the highly accelerated annular supersonic flow with the central subsonic flow above the normal shock. Such velocity structure causes partial collapse and/or oscillation of the eruption column. We propose a regime map showing the diverse flow patterns of eruption columns in the parameter space of the flow rate and the crater geometry, and discuss how the flow patterns of eruption columns change as chamber pressure and conduit-crater geometry evolve in the course of typical explosive eruptions.

Keywords: conduit flow, eruption column, numerical model, transition of eruption style

SVC46-16 Room:304 Time:May 25 11:50-12:05

MP radar observation of the explosive eruption of Sakurajima on May 10th, 2014

SATO, Eiichi[1*] ; FUKUI, Keiichi[1] ; SHIMBORI, Toshiki[1] ; ISHII, Kensuke[1] ; TAKAGI, Akimichi[1] ; YAMAUCHI, Hiroshi[1] ; MAKI, Masayuki[2]

[1]Meteorological Research Institute, [2]Kagoshima University

Although it has been recognized that volcanic ash clouds can be captured by weather radars from the late 1960s, the technique to estimate the amount of pyroclastic materials is not established now. On the other hand, MP (polarimetric) weather radar techniques have been rapidly developed in the field of Quantitative Precipitation Estimation (QPE) and Hydrometeor Classification (HC). We are now trying to develope Quantitative Ash Estimation (QAE) techniques by MP radar, however, false echo is one of the obstacles of QAE.

In this research, we tested a method of determination of false echo region by correlation coefficient (ρhv), which represents non-homogeneity of meteorological clutters, to the case of explosive eruption of Sakuraijma on May 10th, 2014. Then, we analyzed frequency distributions of polarimetric parameters in the volcanic plume regions and the false echo regions. As a result, it is considered that the false echo region depended on multiple factors.

Keywords: volcanic plume, MP radar, polarimetric radar, false echo

Japan Geoscience Union Meeting 2015
(May 24th - 28th at Makuhari, Chiba, Japan)

SVC46-17 Room:304 Time:May 25 12:05-12:20

Observations of Sakurajima Volcanic Ash Column with X-band Polarimetric Radar and Ka-band Doppler Radar

MAKI, Masayuki[1*] ; MAESAKA, Takeshi[2] ; TANADA, Toshikazu[2]

[1]Research and Education Center for Natural Hazards, Kagoshima University, [2]National Research Institute for Science and Disaster Prevention

X-band polarimetric radar and Ka-band Doppler radar data from two explosive eruptions of Sakurajima volcano were analyzed to reveal the inner structures of their respective volcanic ash columns. The first case analyzed was the eruption that occurred on August 18, 2013. The ash column height during that event was 5.5 km above the crater, and falling ash hindered surface traffic visibility in the downtown area of Kagoshima City, which is located about 13km west of the Showa crater. A linear interpolation in time and space was applied to the X-band polarimetric radar data, with 5-minute intervals and 12-tilt elevation angles, to construct a three-dimensional distribution of the radar parameters with a one minute interval and a 250m spatial resolution. The three-dimensional distribution of reflectivity in the ash column reveals a non-uniform structure; the ash column consists of several reflectivity cores which correspond to individual explosions. The pyroclastic material ascent speed, detected from Doppler velocity analysis, was about 60 ms-1 just above the crater. Analyses of reflectivity, differential reflectivity, and co-polar correlation coefficient suggest that the uniformity of ash particle size distribution and particle shape proceeds due to a size sorting mechanism in the ash column when it is moving in a down-wind direction. In the second eruption analyzed, which occurred on May 10, 2014, the ash column reached a height of 4500m above the crater. This eruption was observed by a Ka-band research Doppler radar, set up 3.6km from the crater, and an X-band operational polarimetric radar. RHI scanning of the ash column with the Ka-band radar showed it to have a fine kinematic structure.

Keywords: Weather radar, Ka-band radar, volcanic ash column, reflectivity, Doppler velocity, size sorting

SVC46-P01 Room:Convention Hall Time:May 25 18:15-19:30

Experimental simulation of mixing processes of crystal-rich and -free magmas

KOMAMIYA, Chizen[1*] ; OKUMURA, Satoshi[1] ; NAKAMURA, Michihiko[1]

[1]Department of Earth Science, Graduate School of Science, Tohoku University

Volcanic and plutonic rocks often show textural and petrological evidence on mixing of magmas with different chemical composition and temperature. Several experimental studies have been performed to reproduce textures found in natural rocks and to reveal the mechanism of magma mixing (e.g., Kouchi and Sunagawa, 1982; De Campos et al., 2008, 2011; Laumonier et al., 2014). Important processes that control magma mixing are crystallization and melting of crystals in magmas because they strongly change magma viscosity (Laumonier et al., 2014). For example, when magmas with different temperature contact and mix, crystallization and melting of crystals which are induced by thermal interaction are expected to occur in a hotter magma and in a colder magma, respectively. In addition, the crystallization in a hotter magma is enhanced by shear flow (e.g., Vona and Romano, 2013).

In this study, we experimentally simulated mixing processes of crystal-rich and -free magmas by using an image furnace. In experiments, crystal-rich rock samples with ˜5 mm in an outer diameter (trachyandesite lava from Rishiri volcano and dacite lava from Unzen volcano) were contacted with a crystal-free glass, and then the samples were heated and twisted in the furnace. We used a glass sample synthesized from alkaline rock (trachyandesite lava) because it has relatively low viscosity even at 1 bar under dry conditions. The mixing experiments in the furnace were performed at a temperature of ca. 1100 ℃ (hot spot) under a shear rate of 4.2×10^{-2} s^{-1}. The samples were twisted for 6, 30, and 60 minutes. Because the glass sample synthesized at a temperature of 1400 ℃ is an undercooled melt at experimental temperature (1100 ℃), the crystallization of the melt is expected to occur, and this simulates cooling and crystallization of a hotter magma during magma mixing. After experiments, quenched run products were observed using optical and scanning electron microscopes.

In mixing experiments of the trachyandesite rock and the glass sample, the melting of crystals in crystal-rich magma was observed, while plagioclase crystallizes in crystal-free melt at the boundary of crystal-rich and -free magmas. The mingling between crystal-rich and -free magmas started to be found after 30 min. The mingling seems to enhance the crystallization in crystal-free magma. In a run product of a 60 min experiment, the part of originally crystal-free magma was highly crystallized. The experimental results indicate that the mingling between crystal-rich and -free magmas starts when melt fraction in the crystal-rich magma is high enough to cause the mingling, and it enhances the crystallization of originally crystal-poor magma, which results in rapid increase of magma viscosity. In contrast, the mingling was found only at a 60 min experiment for mixing experiments of the dacite rock and the glass sample. This difference between trachyandesite and dacite rocks may indicate that the onset of the mingling is controlled by the combination of crystal content in crystal-rich magma and the viscosity ratio of melt phases. Our experiments imply that the coupled effect of crystallinity change and mingling controls the mixing of magmas with originally different crystallinity, that is, different chemical composition and temperature.

Keywords: Magma mixing, Magma mingling, Shear flow, Crystallization, Viscosity

Japan Geoscience Union Meeting 2015
(May 24th - 28th at Makuhari, Chiba, Japan)

SVC46-P02 Room:Convention Hall Time:May 25 18:15-19:30

Pre-eruptive conditions and eruptive process of the Tsurumi-dake summit lava; constraints from hornblende phenocrysts

NAGASAKI, Shiho[2] ; ISHIBASHI, Hidemi[1*] ; TAKEMURA, Keiji[3]

[1]Grauate School of Science, Shizuoka University, [2]Faculty of Science, Shizuoka University, [3]Graduate School of Science, Kyoto University

Textural and chemical analyses were done for hornblende phenocrysts in Tsurumi-dake summit lava to constrain its pre-eruptive conditions and eruption processes. Tsurumi-dake summit lava, the latest lava erupted at 7.3-10.5ka (Fujisawa et al., 2002), is andesitic with ca. 30 vol.% of phenocrysts consisting of plagioclase, hornblende, pyroxenes, quartz, biotite and Fe-Ti oxides. Among 566 grains of hornblende phenocrysts observed, 503 grains are completely decomposed. We quantified degree of hornblende breakdown (DHB) by image analyses of BSE images for remaining 62 grains incompletely decomposed. DHB varies from 18 to 98 %.

Chemical analyses were done for incompletely decomposed hornblende grains by using EPMA (JEOL-8800R) at Earthquake Research Institute, University of Tokyo. Most of hornblende phenocrysts are chemically homogeneous. They are divided into two groups based on AlT [= number of Al per 23 oxygens] with ca. 1.2 and 2.1, respectively. negative correlation is observed between AlT and Si content and DHB increases with Si content. All of analyzed hornblende show Al# [=[6]Al/ AlT] lower than 0.21 and satisfy criterion for applying hornblende geothermobarometer of Ridorfi et al. (2010). Using the geothemobarometer, equilibrium pressure and temperature conditions are estimated for hornblende. The estimated pressures show two separated ranges of ca. 100-200 and ca. 350-450 MPa, corresponding to depths of ca. 2.5-5 and ca. 8.5-11km, respectively. Estimated temperatures are ca. 820-920 and ca. 970-1000 degree C for low-P and high-P hornblende phenocrysts, respectively. DHB tends to increase as estimated temperature decreases.

Present results indicate that there were at least two separated magma reservoirs at depths of 2.5-5 and ca. 8.5-11km. The depth of the deeper reservoir is consistent with that inferred from geothermal study of Furukawa (2009), implying the reservoir has existed at least since ca. 7-10 ka. On the other hand, depth range of the shallower reservoir is consistent with that of aseismic zone beneath Tsurumi volcano reported in Ohkura et al. (2002). The consistency may imply that the shallower reservoir contributed to form the aseismic zone.

Coexistence of hornblende phenocrysts with different P-T conditions is consistent with that the lava was formed by magma mixing as pointed out by Ohta et al. (1990, 1991). Mixing of high-T and low-T magmas derived from deeper and shallower reservoirs induced rapid decomposition of low-P hornblende due to heating, but decomposition of high-P hornblende was insignificant because of mixing-induced cooling. High-P hornblende was decomposed during eruption due to degassing. Absence of low-P hornblende with low DHB indicates that post-mixing crystallization was insignificant and eruption occurred right after magma mixing.

Keywords: hornblende, Tsurumi-dake, geothermobarometry, magma chamber

Japan Geoscience Union Meeting 2015
(May 24th - 28th at Makuhari, Chiba, Japan)

SVC46-P03 Room:Convention Hall Time:May 25 18:15-19:30

Zoning pattern analyses of plagioclase phenocrysts in Fuji-Jogan magma; constraints on pre-eruptive magma process

MIWA, Haruna[2] ; ISHIBASHI, Hidemi[1*]

[1]Guraduate School of Science, Shizuoka university, [2]Faculty of Science, Shizuoka University

Jogan eruption occurred at 864-866 at northwest flank in the largest historical eruption of Fuji Volcano. During the eruption, more than 1.3km3 of relatively homogeneous differentiated basaltic lava was effused. In addition, most of the lava was effused in the first two month of the eruption duration, indicating contribution of large magma reservoir. Our interest is in the pre-eruption processes in its magma reservoir.

Plagioclase composition sensitively depends on coexisting melt compositions, melt water content, temperature and pressure. In addition, compositional zonation is not significantly modified due to slow CaAl-NaSi diffusion in plagioclase. These characteristics allow us to decipher magma processes such as crystallization, magma mixing and eruption from compositional zonation of plagioclase phenocrysts. In this study, we focused on compositional zoning patterns of plagioclase phenocrysts in the Jogan basaltic rocks to decipher pre- eruption processes the magma experienced in its reservoir

In this study, plagioclase phenocrysts in two basaltic ejecta, Nagaoyama lava and Nagaoyama scoria, are investigated. BSE images were acquired for 187 and 87 plagioclase phenocrysts in Nagaoyama lava and Nagaoyama scoria, respectively, by using SEM at Michibayashi lab., Shizuoka University. We classified plagioclase phenocrysts into five groups based on gray scale intensity zoning patterns. In addition, chemical analyses were done for representative grains by using EPMA (JEOL 8800R) at Earthquake Research institute, University of Tokyo.

Comparison of BSE image and compositional map indicates that An content [=Ca/(Ca+Na]] is responsible for gray scale intensity in BSE images. Plagioclase phenocrysts in Jogan basalt are classified into the following five groups; (A) normally zoned grains with An-rich homogeneous core, (B) grains showing narrow, strong reverse zoning at boundary between An-poor core and normally zoned rim, (C) oscillatory zoned grains, (D) grains with irregular zoning pattern, and (E) homogeneous grains. Type D and E grains are rare and Type B grains are most abundant. We cannot find grain with reverse zoned rim. Core of type A grain shows An content higher than that observed in any part of type-B grain. Wavy boundary and alignment of melt inclusions are observed at core-rim boundary in type B plagioclase.

Monotonous crystal growth explains normal zonation shown in Type A phenocrysts. Magma mixing is required to explain zoning pattern in type B grains; An-poor homogeneous plagioclase was once melted by magma mixing and then overgrown with An-rich composition to form Type B phenocrysts. Textures observed at core-rim boundary is consistent with this interpretation. Repeated magma mixing and crystallization formed type-C grains. Presence of oscillatory zoned plagioclase indicates that magma replenishment, crystallization, crystal fractionation and eruption have been repeated in this magma reservoir. With considering high effusion rate of basaltic magma in the 864-866 eruption, the reservoir was one of main long-lived ones in Fuji Volcano. Normal zoned rim parts observed in most of plagioclase phenocrysts were interpreted to form during eruption because no discontinuity in zoning pattern is observed in this parts. In type B plagioclase, the rim part is neighboring with reverse zoned part formed by magma mixing, suggesting that eruption occurred right after magma mixing.

Keywords: Fuji volcano, plagioclase, Compositional zoning, magma chamber, Jogan eruption

Japan Geoscience Union Meeting 2015
(May 24th - 28th at Makuhari, Chiba, Japan)

SVC46-P04 Room:Convention Hall Time:May 25 18:15-19:30

Groundmass texture of B-fall deposit from the Ten-nin eruption, Asama volcano, Japan

HONGO, Yuko[1] ; NAKAMURA, Michihiko[1] ; OKUMURA, Satoshi[1*] ; MUJIN, Mayumi[1]

[1]Department of Earth Science, Graduate School of Science, Tohoku University

Volcanic eruptions often show the transition from explosive to non-explosive activities and the change in the explosivity during explosive activity. A controlling factor of the explosivity is the magma ascent velocity in volcanic conduits (e.g. Jaupart and Allegre, 1991). When the velocity of magma ascent is high, magma does not experience gas loss, which results in explosive activity. On the other hand, non-explosive eruption is caused if magma ascent velocity is low and efficient outgassing occurs. In this study, we investigated crystal size distribution (CSD) of plagioclase microlite because it reflects magma decompression rate. We measured the CSD in fallout pumices from the Ten-nin eruption of Asama volcano and compared the CSD with those of other eruptions. The fallout deposit of the Ten-nin eruption is divided into eight subunit layers from B-1 to B-8. Four layers (B-2, B-4, B-6 and B-8) are composed of gray and brown pumices, while other layers, i.e., B-1 and B-5, and B-3 and B-7, are formed by volcanic ash and dense lithic fragment, respectively. The B-4, B-6 and B-8 also contain dense lithic fragment. All the samples investigated in this study have a common bulk chemical composition (Hongo et al., Volcanological Society of Japan, 2013). We analyzed bulk density and CSD for the pumices from B-4, B-6 and B-8. To obtain the CSD, we corrected the effect of microlite shape using CSD Slice5 software (Morgan and Jerram, 2006) and CSD corrections software (Higgins, 2000) after measurement of the length and number of the microlites on backscattered electron images with 800 magnifications. The vesicularities and crystallinities of B-4 and B-6 were smaller than those of B-8. The CSD slope was slightly steeper than those of B-4 and B-6. We compared the CSD obtained in this study with those of explosive to non-explosive eruptions reported by previous studies. The CSD data show that the slopes of the explosive eruptions are generally steeper than those of the non-explosive ones. This result implies that the CSD slope reflects magma ascent velocity and eruption style, but we need more data to clarify the relationship between CSD and eruption style, since no clear difference was found in some CSDs of sub-Plinian and lava dome eruptions (e.g. Castro and Gardner, 2008).

Keywords: crystal size distribution, microlite, pumice, sub-Plinian eruption, Asama volcano

Japan Geoscience Union Meeting 2015
(May 24th - 28th at Makuhari, Chiba, Japan)

SVC46-P05 Room:Convention Hall Time:May 25 18:15-19:30

Development process and controlling factors of bubble waves in bubbly flow

KINOSHITA, Akane[1*] ; TORAMARU, Atsushi[2]

[1]Department of Earth and Planetary Sciences, Graduate School of Sciences, 33 Kyushu University, [2]Department of Earth and Planetary Sciences, Faculty of Sciences, 33 Kyushu University

The hydrodynamic behavior of a two-phase system is investigated by an analog experiment. Bubbly flows with spatially periodic distribution of bubbles are sometimes observed in various natural situations such as in the conduit and lava flow. For instance, the early stage of the 1986 fire fountain eruptions of the Izu-Oshima volcano had the continuous magma effusion with a rhythm of mean period about 5s. This suggests the inhomogeneous distribution of bubbles in the conduit. The similar structure of bubble distributions is observed in a glass of Guinness beer. The bubbles are distributed nearly uniformly at the moment Guinness beer is poured, and quickly form layers or waves which appear to propagate downward. Unfortunately, Guinness is not appropriate for scientific experiment because of difficulties to control parameters (e.g. volume fraction and radii of bubbles), formation and dissolution of bubbles, and poor reproducibility of initial conditions such as pouring condition. We therefore conducted an analog experiment using the special liquid and the hollow glass particles as analog materials of a beer liquid and bubbles, respectively, presuming that the bubble waves in Guinness form by the relative motion of bubbles to liquid by buoyancy, but not by the formation and dissolution processes. We mixed the liquid and the particles in cylindrical test tube by gently shaking the test tube. The bubble segregation or relative upward migration of bubbles starts from the homogeneous mixture as an initial state just after stopping shaking. We found that under some conditions, the bubble waves form during the upward segregation of bubbles. In order to constrain factors for the formation of bubble waves, we conducted the series of experiments with varying the volume fractions, sizes of bubbles and the inclination of a test tube. We found that the bubble waves formed only when we incline the test tube, and when volume fractions of the particles are less than approximately 30 %. If we settled the test tubes vertically, the bubble waves didn't form. On the other hand, when we inclined the test tubes, we observed that the circulatory current of the particles directed upwards near the inter surface at higher wall of the test tube and downwards near the lower wall of it. The wave like structure of the particles with the wave length about 10-20 mm and the horizontal width about ~5mm developed near the lower wall of the inclined test tube. The wave length and the horizontal width of bubble waves were inversely proportional to the inclined angle of the test tube and the volume fraction of the particles. We propose the formation mechanism of bubble waves on the basis of the Kelvin-Helmholtz instability which develops at the thin boundary layer formed near the lower wall, where the downward bubble-poor and overlaid upward bubble-rich layers contact each other.

Keywords: bubbly flow, inhomogeneous distribution of bubbles, analog experiment

SVC46-P06 Room:Convention Hall Time:May 25 18:15-19:30

Direct molecular dynamics simulations of homogeneous bubble nucleation and improvements of classical theory

TANAKA, Kyoko[1*] ; TANAKA, Hidekazu[1] ; DIEMAND, Juerg[2] ; ANGELIL, Raymond[2]

[1]Institute of Low Temperature Science, Hokkaido University, [2]University of Zurich

Bubble nucleation in liquid is a liquid-to-vapor transition phenomenon and plays an important role in vulcanism. Studies of homogeneous liquid-vapour nucleation typically use the classical formula (CNT) for the bubble nucleation rate. However, the applicability of the CNT is not well understood.

Numerical techniques such as molecular dynamics and Monte-Carlo simulations are powerful methods to resolve details of the nucleation process and provide useful test cases for nucleation models. Typically, these simulations show large deviations from the CNT predictions. Most of the simulations for bubble nucleation in the literature use around 10^5 or fewer atoms, making it difficult to measure nucleation rates directly.

Recently, we presented large-scale, micro-canonical molecular dynamics simulations of homogeneous bubble nucleation with $5 * 10^8$ Lennard-Jones atoms, and succeeded to directly measure nucleation rates in the range of $10^{21-25}\mathrm{cm}^{-3}\mathrm{s}^{-1}$ for argon by resolving bubble nucleation events in the steady state nucleation phase [1,2]. The unprecedented size of the simulated volumes allows us to resolve the nucleation and growth of many bubbles per run in simple direct micro-canonical (NVE) simulations while the ambient pressure and temperature remain almost perfectly constant.

We find bubble nucleation rates which are lower than in most of the previous, smaller simulations. It is widely believed that classical nucleation theory (CNT) generally underestimates bubble nucleation rates by very large factors. However, our measured rates are within two orders of magnitude of CNT predictions - only at very low temperatures the CNT underestimates the nucleation rate significantly.

We also derive an improved classical formula for the homogeneous bubble nucleation rate, where we revise the prefactor in the nucleation rate and compare it with the widely used classical nucleation theory (CNT) [3]. Our large-scale molecular dynamics simulations and laboratory experiments for argon bubble nucleation enable us to precisely test our theoretical models. The improved formula including the Tolman correction with a small positive Tolman length leads to good agreement with both MD simulations and laboratory experiments.

[1] J. Diemand, R. Angelil, K. K. Tanaka, and H. Tanaka, Pys. Rev E 90, 052407 (2014)
[2] R. Angelil, J. Diemand, K. K. Tanaka, and H. Tanaka, Pys. Rev E 90, 063301 (2014)
[3] K. K. Tanaka, H. Tanaka, R. Angelil, and J. Diemand, submitted

Keywords: bubble nucleation, liquid to vapor transition, phase transition, molecular dynamics simulation

SVC46-P07 Room:Convention Hall Time:May 25 18:15-19:30

Numerical analysis of the behavior of a viscoelastic body containing gas bubbles by rapid decompression

KUROKAWA, Noriaki[1*] ; KAMEDA, Masaharu[1] ; ICHIHARA, Mie[2]

[1]Mech. Sys. Eng., TUAT, [2]ERI, Univ. of Tokyo

Brittle fragmentation of vesicular magma is considered to be a trigger of explosive volcanic eruptions. Ichihara and Rubin (2010) defined the brittleness as a dominant parameter of the brittle fragmentation of magma. They concluded that the brittle fragmentation occurred when the brittleness of magma was close to unity. Kameda et al. (2013) reported that the brittle-like fragmentation occurred in their laboratory experiments even if the brittleness of specimen was lower than unity. They suggested that the brittle-like fragmentation was initiated by the crack developed from the interior of the specimen due to non-uniform spatial distribution of bubbles. After the partial fragmentation occurs, the rapid decompression around the fracture surface induces sequential fragmentation events.

In this study, to verify the scenario of the brittle-fragmentation proposed by Kameda et al., we simulated numerically the behavior of a Maxwell viscoelastic body including a few bubbles due to rapid decompression. We examined the evolution of the differential stress and brittleness around the bubbles in viscoelastic body.

We used COMSOL multiphysics ver. 5.0 as the platform for our numerical analysis. We employed axial symmetry model as the space dimension, and generalized Maxwell viscoelastic model as the viscoelastic model. In the first case (Case 1) of our calculation, we set the calculation area as a hemisphere (a quarter of a circle which radius was 100 mm), and arranged two spherical bubbles in the area. The large bubble (radius is 20mm) was located at the central point of the hemisphere. Another small bubble (radius is 5 mm) was located at the isolate position beneath the large bubble, and its central point was placed on the symmetry axis of the hemisphere. The physical property of the viscoelastic body and the profile of decompression were the same values as the laboratory experiment. We assumed the internal pressure of bubbles remained a constant value.

In Case 1, the stress concentration is observed at the surface of small bubble facing the large bubble. In contrast, smaller differential stress is observed at the surface of large bubble facing the small bubble. To investigate this reason, we calculated the numerical analyses (Case 2, 3) using the geometry of Case 1. In Case 2, internal pressure was applied only on the large bubble. In Case 3, the internal pressure was applied only on the small bubble. These results showed stress concentration is observed at the surface of small bubble only in Case 2.

We propose the following scenario of stress concentration: There is the influence range on the distribution of differential stress around the bubble. The range spreads as the size of bubble becomes large. If the bubble exists in the influence range of differential stress produced by the other bubble, stress concentration occurs on the surface of bubble.

In Case 4, we calculated the time variation of the brittleness with considering the change of the internal pressure of the bubble due to its expansion. We calculated the stress field around a single bubble placed spherically symmetric position in the domain. The volume of the bubble is equal to the sum of the volume of the bubbles in Case 1. We assumed that the internal pressure of the bubble varied isothermally. The results showed the time variation of the brittleness on the bubble's surface in Case 4 was not so different from Case 1. On the other hand, the maximum value of the differential stress around the bubble was developed steeper in Case 1 than in Case 4. This means that the critical brittleness, which is defined as the brittleness at the time when the maximum differential stress reaches the critical fracture stress, is higher in Case 1 than in Case 4.

In conclusion, (1) Stress concentration occurs at the bubble's surface in the case where neighboring bubbles are close to their bubble radii. (2) The critical brittleness at the position where stress concentration occurs becomes large.

Keywords: Magma, Viscoelasticity, Fragmentation, Numerical analysis

Japan Geoscience Union Meeting 2015
(May 24th - 28th at Makuhari, Chiba, Japan)

SVC46-P08 Room:Convention Hall Time:May 25 18:15-19:30

X-ray CT observation of fragmentation of vesicular magma analogue

AOKI, Yamato[1*] ; KAMEDA, Masaharu[1] ; TSUGO, Mitsuaki[1] ; YAMADA, Akihumi[1] ; ICHIHARA, Mie[2] ; OKUMURA, Satoshi[3] ; UESUGI, Kentaro[4]

[1]Mech. Systems Eng.,TUAT, [2]ERI, Univ. of Tokyo, [3]Earth Sci., Tohoku Univ., [4]JASRI

"Explosive eruption" of volcano adversely affects to our lives. The explosive eruption may be triggered by the rapid discharge of gas in vesicular magma due to its brittle fragmentation. We focused our attention to the "brittle-like fragmentation" (Kameda et al. JVGR 2013) which was defined as the solid-like fracture of the material whose bulk rheological properties was close to fluid state. We tackle to elucidate the mechanism of the brittle-like fragmentation by laboratory experiment.

Recent our laboratory experiment (Shida et al. IAVCEI 2013) showed that the onset of brittle-like fragmentation depended on the size of specimen even if the bulk rheological properties and void fraction remained constant. The probability of the fragmentation decreases as the size decreases. In our experiments, the heterogeneity of spatial and size distribution of the bubbles was more remarkable in larger specimen than in smaller one. We guess that this heterogeneous distribution of the bubble in the specimen is a main source of the brittle-like fracture.

On observing the behavior of the fracture, we use the syrup as magma analogue. The syrup is suitable for the magma analogue because its rigidity is close to the rigidity of magma, and its viscosity is varied widely by hydration or dehydration. Furthermore, we add H_2O_2 and MnO_2 into the syrup and generate O_2 gas bubbles to mimic the vesicular magma. We use the rapid decompression equipment to observe the fracture of the specimen. It consists of the pressure container whose top is sealed by plastic (Lumirror) film. A thin nichrome wire is bonded to the film. We set the specimen in the pressure container, and pressurize the container by filling nitrogen gas up to our desired value. After pressurization is completed, we energize the nichrome wire by rapid current discharge from capacitor. The film is abruptly ruptured by the heat of the nichrome wire, then rapid decompression attacks the specimen. The specimen has a hemispherical shape whose diameter is about 20mm. We choose the viscosity of each specimen in the range from 10 MPa s to 200 MPa s. The initial pressure before decompression is 2 MPa. The characteristic time of decompression (the time when the pressure in the container reach 1/e of the initial value) is about 5 - 7 ms.

We conducted the X-ray micro CT imaging at BL20B2 in SPring-8 (JASRI) to observe the internal structure of the specimen. We took the transmission images of the specimen whose viewing angle was varied from 0 to 180 degrees every 0.1 degree. Each captured image has 2048 pixels in width and 1400 pixels in height. We conducted the CT imaging before compression, after compression, and after rapid decompression (at atmospheric pressure). We also captured the dynamic behavior of the specimen during decompression by high-speed radiography (100 fps).

From these experiments, we found that the fracture occurred at the parts where the large bubbles were accumulated. In contrast, the fracture did not occur at the parts where a large bubble independently existed. Furthermore, we found that the fracture may occur when the inter-distance of neighboring bubbles is close to the order of the bubble radius, even if the rheological bulk properties of the specimen is close to the fluid state (the brittleness is not near unity).

Keywords: Magma, Fragmentation, Rapid decompression, Brittleness, X-ray CT, Non-uniform distribution of bubbles

Japan Geoscience Union Meeting 2015
(May 24th - 28th at Makuhari, Chiba, Japan)

SVC46-P09 Room:Convention Hall Time:May 25 18:15-19:30

Estimating of the maximum volume of magma accumulation in the crust before a large volcanic eruption

FUJITA, Shiori[1*] ; SHIMIZU, Hiroshi[2]

[1]Department of Earth and Planetary Sciences, Graduate School of Sciences, Kyushu University, [2]Institute of Seismology and Volcanology, Faculty of Sciences, Kyushu University

Massive volcanic eruption, which emits several hundred cubic kilometres of magma and often forms huge calderas afterwards, occurs around once in every 10000 years in Japan. Although it is necessary for a huge amount of magma to accumulate in the crust for such a big eruption, there has been little quantitative analysis to determine the critical value of mechanical magma accumulation in relation to the depth and shape of the magma chamber and magma accumulation rate.

While the long-term magma accumulation rate at the volcano was estimated to be about 0.001-0.01km^3/yr inferred from the magma volume of past eruption, Druitt et al. (2012) suggest the possibility that a massive store of about 10km^3 magma had accumulated for around just 100 years before the eruption, based on an analysis of Mg concentration in plagioclase crystals of Santorini pumices. This result indicates an extraordinarily large magma accumulation rate of 0.05-0.1km^3/yr, and recently such a huge rate has actually been observed in some volcanoes. For instance, Chang et al.(2010) obtained a magma accumulation rate of 0.06-0.07km^3/yr in 2005-2008 from GPS and InSAR survey at Yellowstone caldera. InSAR observation also indicated a magma accumulation rate of 0.03km^3/yr at Uturuncu volcano in Bolivia (Sparks et al.2008). These research results show that in some cases magma is able to move abruptly upward and accumulate for a term of at least 100 years. Because the stress relaxation time of the crust as viscoelastic body is much longer than this time scale, the response of the crust to such a speedy magma accumulation can be treated as elastic deformation.

In this study, we posit the volume of magma accumulation in the crust which is possible over a time period shorter than the stress relaxation time of the crust. We calculate crustal deformation, strain and stress based on several magma chamber's depth, shape and volume pattern, and compare these with the limit strain of the crust. We presumed the shape of the magma chamber to be a sphere, dyke, or sill with a depth of several to a dozen kilometers. We used the crustal deformation calculation model for an elastic body proposed by Okada (1992).

We assumed a spherical magma chamber 10km deep and a volume change of 10km^3 when the magma accumulation rate is huge, and therefore the crust is regarded as a perfect elastic body. In this case, the strain value exceeded the crustal limit strain of 10^{-4} within a 30 km radius. This result indicates the crust around magma chamber yields and plastic deform before 10km^3 accumulation or causes brittle fracture as to a spherical magma chamber 10km deep.

Keywords: large volcanic eruption, magma accumulation, crust, strain, stress, caldera

Japan Geoscience Union Meeting 2015
(May 24th - 28th at Makuhari, Chiba, Japan)

SVC46-P10 Room:Convention Hall Time:May 25 18:15-19:30

Parameterization of conduit flow model based on the inverse analysis of data from ground deformation and magma extrusion

MATSUO, Naoya[1*] ; KOYAGUCHI, Takehiro[1] ; SUZUKI, Yujiro[1]

[1]Eartuquake Research Institute, The University of Tokyo

During volcanic eruptions, slight changes in geological conditions often result in various types of eruptions such as effusive and explosive eruptions. In order to understand such complexities of conduit flow dynamics, several conduit flow models have been proposed (e.g., Melnik and Sparks, 2005). In the conduit flow models, temporal evolution of pressure and velocity in the conduit are calculated from model parameters such as volume of magma chamber and magma properties. In order to forecast the transitions of eruptions, these model parameters need to be estimated from the inverse analysis of time-series data of observation. Anderson and Segall (2013) formulated a posterior probability density function of model parameters given ground deformation and magma extrusion data based on Bayes' theorem, and yielded probabilistic estimates for the model parameters using a Markov Chain Monte Carlo (MCMC) algorithm. However, because their inverse analysis includes many model parameters, it is difficult to understand the influence of each observation on the parameter estimation. The present study aims to systematically investigate the influence of ground deformation and magma extrusion data on parameter estimation, and ultimately, to estimate model parameters of a more sophisticated conduit flow model that takes into account the effects of gas escape and crystal growth during magma ascent (e.g., Kozono and Koyaguchi, 2012).

In this study, a model consists of the magma plumbing system where pressure of a spherical magma chamber in elastic rocks is determined by the balance between magma influx and outflux. We also assume that conduit flow is determined by the balance between pressure gradient and viscous force (i.e., Poiseuille flow). In this system, model parameters include chamber volume, conduit length, effective elastic modulus of magma in the chamber and the chamber itself, conduit radius, magma density and viscosity. On the other hand, observables include the time-series data of the volume change due to inflation/deflation of the chamber (ΔV_G) and the amount of extruded magma (ΔV_E).

Assuming that magma density and viscosity are constant in the conduit, extrusion rate Q and magma chamber pressure P approach the steady solution (Q_s,P_s) with a time constant τ. A parameter τ is determined by chamber volume, effective elastic modulus, magma viscosity, conduit radius and conduit length. In the case where τ can be estimated from the time-series data of ΔV_G and ΔV_E, the estimated value of τ provides the information related to the conductivity of the conduit flow and the system size, whereas the difference between ΔV_G and ΔV_E provides the information related to magma compressibility and the shape of the chamber.

We have also preliminarily investigated the influence of gas escape and crystal growth on the parameter estimation assuming various function forms for magma density and magma viscosity. In this preliminary study, we compare the probability density distribution of model parameter estimated numerically using a MCMC algorithm with the analytical results in order to understand how the parameter estimation using MCMC algorithm is applicable to the problems of complex conduit flows with gas escape and crystal growth.

Keywords: volcanic eruption, conduit flow, lava dome, ground deformation, inverse analysis

Japan Geoscience Union Meeting 2015
(May 24th - 28th at Makuhari, Chiba, Japan)

SVC46-P11 Room:Convention Hall Time:May 25 18:15-19:30

Sawtooth wave-like pressure change and cyclic out-gassing observed in laboratory experiments

KANNO, Yo[1*] ; ICHIHARA, Mie[1]

[1]The Earthquake Research Institute, the University of Tokyo

1.Introduction

A sawtooth wave-like (SWT) pressure change was observed in laboratory syrup eruption experiments (Kanno and Ichihara, 2014,VSJ fall meeting).

Sawtooth wave-like infration-defration cycles have been observed with eruptions at many volcanoes (Genco and Ripepe 2010, Lyons et al. 2012, Nishimura et al 2013). We expect that clarifying the mechanism of a similar oscillation in this experiments helps understanding the actual volcanic phenomena. Conduit flow patterns are controlled by the gas volume fraction and relative velocity between liquid and gas (Vergniolle and Jaupart, 1986). Supposing that the SWT pressure oscillation was generated by transitions of flow patterns, we conducted experiments on flow in a tube with varying fluid rheology and injected gas flux. However we never observed the SWT oscillation.

In this study, we examine effects of the chamber below the tube on generation of the SWT oscillation.

2.Equipment and Method

Gas is injected to a transparent tube to generate alternate layered flow of syrup and gas. The viscosity of the syrup is about 1 Pa.s. The diameter of the tube is 5 mm. An acrylic chamber (ϕ=50 mm, H=100 mm) is attached beneath the tube. A pressure transducers is mounted at the injection point in the tube and another at the bottom of the chamber. In addition, a microphone is mounted at the exit of the tube. Flow in the tube is recorded with a high-speed camera (Fig.1a).

We inject the syrup in the tube to the height of 60 mm from the bottom of the tube. In order to keep the syrup within the tube, we use a 800-mm long tube. We partially fill the chamber with water and control the volume of the chamber (Vc) by changing the amount of water. Injected gas flux (Qin) is controlled by a regulator.

3.Result

We control Vc from 0 to 120 cm^3 and Qin from 0.1 to 30 $\mu m^3/s$ for each Vc.

(1) Changing Vc with constant Qin

For small values of Vc, quasi-sinusoidal pressure oscillation is observed with periodic ruptures of syrup layers at the top. The velocity and the thickness of the following syrup layers are nearly constant with a minor influence of the rupture.

The SWT oscillation is observed for sufficiently large Vc (Fig.1b). In this case, all syrup layers burst simultaneously to make pressure drop. After this event, syrup layers recover with deformation of syrup film flowing down the inner wall, and the pressure in the chamber starts to increase gradually. The syrup layers are accelerated with the pressure increase and their thicknesses become thinner. Then, the syrup layers burst again to cause pressure drop.

(2)Changing Qin with constant Vc

When Vc is small, quasi-sinusoidal pressure oscillation is observed in all the experimental range of Qin. The period of the oscillation is smaller when Qin is larger. When Vc is sufficiently large, the SWT oscillation appears intermittently among the quasi-sinusoidal oscillation. The SWT oscillation dominates when Qin further increases.

4.Discussion

For volcanic systems, asymmetric pressure change has been explained by a coupling mechanism among pressure in a magma chamber, conduit flux, and viscosity (Ida,1996; Barmin et al,2002; Nakanishi and Koyaguchi,2008).

Based on these models, we considered two effects:

(1) Viscous dissipation in the tube becomes larger (smaller) when the thicknesses of the syrup layers increase (decrease).

(2) The chamber plays a role of a buffer.

With these assumptions, the experimental system is formulated by simple ordinary differential equations.

This model generates a SWT pressure change with increasing Vc at constant Qin (Fig.1c). When Vc is small, quasi-sinusoidal pressure oscillation is generated. For constant Vc, the waveform gradually changes from SWT to quasi-sinusoid with decreasing Qin.

In this way, the model can qualitatively simulate the oscillation patterns that are observed in the laboratory experiments. In the future, we will study effects of each parameter in more detail.

Keywords: Sawtooth wave, Analog experiment, Multi phase flow, Magma chamber, Conduit flow, Tilt motion

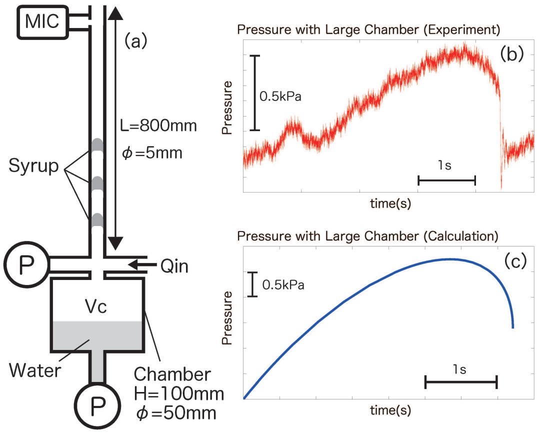

Japan Geoscience Union Meeting 2015
(May 24th - 28th at Makuhari, Chiba, Japan)

SVC46-P12 Room:Convention Hall Time:May 25 18:15-19:30

Variation of VLP signals accompanying eruptions at Stromboli volcano, Italy

YAMADA, Taishi[1*] ; AOYAMA, Hiroshi[1] ; NISHIMURA, Takeshi[2] ; KAWAGUCHI, Ryohei[3] ; MIWA, Takahiro[3] ; FUJITA, Eisuke[3] ; RIPEPE, Maurizio[4] ; GENCO, Riccard[4] ; LACANNA, Giorgio[4]

[1]Faculty of Science, Hokkaido University, [2]Graduate School of Science, Tohoku University, [3]National research Instituite for Earth science and Disaster prevention, [4]Dipartimento Scienze della Terra, Universita di Firenze

Stromboli volcano in Italy, one of the most active and famous volcano in the world, has been the target field of volcanology to understand eruption dynamics. From aspect of volcano seismology, broadband seismic observations have revealed that VLP(very-long-period) signals (10~sec) are dominant among the seismic signals accompanying eruptions at Stromboli volcano (e.g. Neuberg et al., 1994). Chouet et al. (2003) demonstrated that inflation-deflation-inflation sequence of moment components, which represent inclined crack, is dominant at VLP signals observed at Stromboli volcano. The estimated force system was considered to represent the rise and ejection of gas slug, which causes repressurization of crack corresponding second inflation. However, most previous researches have analyzed a few VLP events having specific waveform characteristics, that were typical among their temporary observation data for days or weeks.

We have conducted broadband seismic observation at Stromboli volcano since May 2014. From 4 month long broadband seismic record, most VLP events seem to have similar waveform characteristics mentioned in Chouet et al. (2003) (inflation-deflation-inflation sequence). However, we recognized there are several waveform types prior to main first inflation phase.

1. Gradual inflation (10 ~30 sec) prior to main inflation
2. Having small deflation phase (~5 sec) during gradual inflation (type 1)
3. Gradual deflation (10 ~30 sec) prior to main inflation
4. Combination of type 2 and 3
5. Short deflation (~5 sec) prior to main inflation
6. No main inflation phase (Only downward pulse)

As described above, there are certain groups of VLP events which have deflation phase prior to main first inflation phase. Even if amplitude of deflation phase is small, such deflation process cannot be explained by the simple gas slug rising model. Moreover, some VLP events (type 6) have no inflation phase at the onset. Particle motion analysis for onset and first inflation phase shows events in type 1, 2, 5, 6 have common azimuthal direction (NW-SE direction), while events in type 3, 4 have slightly different direction. Since Stromboli volcano has several active vents on the northwest direction from our seismic station, these differences of azimuthal motions may reflect the difference of vents where eruptions were taken place. Another remarkable feature is about the transition of occurrence frequency of each type. For example, occurrence frequency of type 6 has decreased at the beginning of Aug. 2014. Those days correspond to the period that amplitude of RMS (root-mean-square) of high frequency (>3 Hz) has decreased. Also transition of eruption style has been reported at that period, from intermittent Strombolian eruptions to lava outflow and effusive eruptions.

Keywords: Strombolian eruptions, VLP, explosion earthquakes

Japan Geoscience Union Meeting 2015
(May 24th - 28th at Makuhari, Chiba, Japan)

SVC46-P13 Room:Convention Hall Time:May 25 18:15-19:30

Relative hypocenter determination of eruption earthquakes using deconvolution: Application to Stromboli volcano

SUGIMURA, Shunsuke[1*] ; NISHIMURA, Takeshi[1] ; AOYAMA, Hiroshi[2] ; YAMADA, Taishi[2] ; FUJITA, Eisuke[3] ; KAWAGUCHI, Ryohei[3] ; MIWA, Takahiro[3]

[1]Graduate School of Science, Tohoku University, [2]Faculty of Science, Hokkaido University, [3]NIED

Eruption earthquakes are repeatedly observed with intervals of several minutes, hours or days associated with Strombolian or Vulcanian explosions. These eruption earthquakes generally have obscure onsets of P or S phases, which disables us to use general hypocenter determination methods using the arrival times of these waves. In this study, we determine relative hypocenter locations of eruption earthquakes associated with repetitive eruption, using deconvolution filter and master event method.

We use records of three tilt meters that are deployed near the active crater of Stromboli volcano since May 2014. We analyze tilt signals of eruption earthquakes that are recorded with a sampling frequency of 100Hz. We relate arrival time difference between a master event and slave event at each station with differences of hypocenter parameters. We use deconvolution filter to obtain arrival time difference because eruption earthquakes observed at each station have similar waveforms. However, since the origin time of the master event is not known, we further calculate time differences of the arrival time differences between two stations to eliminate the origin time difference.

We analyze 31 eruption earthquakes occuring from 0:00 a.m. to 3:00 a.m., July 1of 2014, whose amplitudes are more than 20 micro radian at all the stations. We define the first event as a master event. Assuming the epicenter at NE crater, the depth of 100m for master event, and the wave velocity of 800m/s, we determine relative depths of slave events using least squares methods. The results show that the relative depths are estimated to be from 70 to 225m.

Deconvolution filter enables us to automatically read the time differences of arrival time differences between two stations. By analyzing large number of data, we will be able to monitor the spatio-temporal change of the source locations of repetitive eruptions.

Keywords: hypocenter determination, eruption earthquake, master event method, deconvolution, Stromboli volcano

Japan Geoscience Union Meeting 2015
(May 24th - 28th at Makuhari, Chiba, Japan)

SVC46-P14 Room:Convention Hall Time:May 25 18:15-19:30

NW-SE trending graben structure and crater row on Teishi Knoll, off Izu Peninsula

MINAMI, Hiroki[1*] ; IWABUTI, Yo[1]

[1]Hydrographic and Oceanographic Department, Japan Coast Guard

Teishi knoll, located 4 km off eastern Izu Peninsula, is submarine volcano of the Higashi-Izu monogenetic volcano group. Hydrographic and Oceanographic Department of Japan Coast Guard (JHOD) monitors and surveys the maritime and submarine volcanoes in Japan and we conducted bathymetric survey of Teishi knoll with survey vessel and autonomous underwater vehicle (AUV). Though intensive bathymetric surveys were done after the 1989 eruption by JHOD (Oshima et al., 1991), the resolution of used echo sounder was lower than the latest one and the detailed morphology was not mapped. Our survey revealed that NW-SE trending graben structure formed on the Teishi knoll. In addition, four small craters were aligned with same NW-SE trending as graben. These surface deformations such as graben and crater row indicate behavior of magma in the subsurface.

1. Method

The survey was conducted in December 2014. Multibeam echo sounder EM302 installed on S/V Kaiyo and interferometric sonar GeoSwath Plus on AUV GondouS were used.

2. Result

The graben formed just southeast of the main crater. The length is 120 m, width 70 m and 1.5 m deep. The four small craters formed inside the main crater associated with 1989 eruption. The craters are aligned in the NW-SE direction and each crater has 20?50 m in diameter. NW-SE trending linear topographic high also formed between the graben and craters.

3. Interpretation

Yamamoto et al 1991 concluded that magma intrusion into the sediment blanket caused the eruption, vapor explosion. Okada and Yamamoto 1991 concluded that the tensile fault, N125E strike (?NW-SE) caused the magma intrusion to sedimentary layers. The relationship between magma intrusion and surface deformation and the depth of the top of the dike is approximately equal to half the width of graben (Mastin and Pollard 1988; Chadwick and Embley 1998). The relationship was applied to our result in the Teishi knoll. The graben width 70 m implies that the top of the dike beneath the graben was at about 35 m depth. There are no direct evidences that the graben formed associated with 1989 eruption. Considering that the crater row is aligning in same NW-SE direction, same width 70 m and lying on the same line as graben, the graben might be formed in the identical environment, that is 1989 eruption with dike intrusion.

Keywords: Higashi-Izu monogenetic volcano group, bathymetry, multibeam echo sounder, graben, crater row, dike

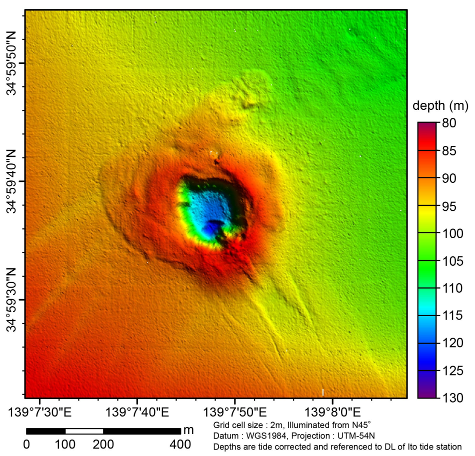

Japan Geoscience Union Meeting 2015
(May 24th - 28th at Makuhari, Chiba, Japan)

SVC46-P15 Room:Convention Hall Time:May 25 18:15-19:30

Variety of morphologies which are formed by molten lava-water interaction

NOGUCHI, Rina[1*] ; KURITA, Kei[1]

[1]Earthquake Research Institute, the University of Tokyo

There exists 2 types of responses when molten lava interacts with water environment: explosive and non-explosive. However, during eruption, it is difficult to make a judgment on whether explosion occurs or not. For example, in Nornahraun, Iceland, lava flowed into a river, but no explosion occurs to this day. This is a same as Nishinoshima Island. However, previous studies presented explosions which relate with lava-water interaction occurred in many places including Japan in the past [e.g. Mattox and Mangan, 1997; Ito and Taniguchi, 1996]. Its disaster risk has not been recognized; its explosivity would reach the degree of maar (magma-water interaction), and it is possible to generates low-concentration pyroclastic density current [Fagents and Thordarson, 2007]. Thus, it is important to understand this explosion mechanism for us Japan because of not only interesting of volcanic explosion but also prevention and reduction of disaster when lava flow into water environments near distinct of residence.

Today, it is known that there exists 3 types of morphometry which relates to lava-water interaction: rootless cones, spiracles, and lava pillars.

Lava-water explosive interaction have been well-known in basaltic volcanism, but previous studies showed it occurred in andesitic and rhyolitic [e.g. Hayakawa and Yui, 1989; Ito and Taniguchi, 1996]. Although their related-morphology has been studied, there remains problems to understand this phenomenon. Rootless cone (aka secondary crater and pseudocrater) is a typical morphology which is formed by lava-water interaction. They have a variety of shape; Hamilton et al., 2010 showed 3 archetypes of them which relates to flowing types of lava (tube-, channel-, and broad sheet lobe-fed). However, the relationship between their morphometry and formation conditions (e.g. explosivity, water/magma mass ratio, underlying sediments) has not been revealed. This is a problem for not only rootless cones but also other pyroclastic cones (e.g. scoria cone, maar, tuff cone). Rootless cones would be useful also in planetary science. Recent studies have found candidates of rootless cone on Mars [e.g. Greeley and Fagents, 2001]. These morphologies are expected to reveal recent 100Ma Martian magmatism. Thus this study could give great influence for planetary science. It is necessary to understand the variety of morphology and distribution of rootless cones to know the style of magmatism and environment.

Spiracles are found in bottom of lava flows as irregular shaped-vesicles which are formed by lava-water explosion. In Japan, cylindrical vesicles in Aokigahara lava flow was considered as typical spiracles for many years. Now its are considered as tree molds which were vertically-elongated by inflation of lava, and we lost an image of spiracle. Therefore we should reconstruct the image once again.

Lava pillars are considered as results of non-explosive lava-water interaction [e.g. Gregg et al., 2002]. They show chimney-like morphology, and has been found both in subaerial and submarine volcanism. Recently, Gregg et al., 2002; Gregg and Chirstle, 2013 showed that lava pillars were formed by water vaporization or hydrothermal activity at gaps of pahoehoe lava lobes. However, there exists lava pillars which were formed by a'a lava flow. Hence it remains problems for the lava pillar formation and non-explosive lava-water interaction.

In this presentation, we will review previous studies about morphologies which relate with lava-water interaction, and marshal problems to 1) understand volcanic explosion, 2) know its disaster risks, and 3) apply to planetary science. Especially focusing on rootless cone, we will discuss its variety of shapes based on our aerial photo analysis and field survey. Additionally, a new type of lava-water interaction-related morphology which we found both in Iceland (called as hraunbollar) and Hawaii will be introduced.

Keywords: lava-water interaction, explosion, rootless cone, spiracle, lava pillar

Japan Geoscience Union Meeting 2015
(May 24th - 28th at Makuhari, Chiba, Japan)

SVC46-P16 Room:Convention Hall Time:May 25 18:15-19:30

The influence of the linear increase in the source height on the 1D quasi-steady state fall and sedimentation processes

IRIYAMA, Yu[1*] ; TORAMARU, Atsushi[2]

[1]Department of Earth and Planetary Sciences, Graduate School of Sciences, Kyushu University, [2]Department of Earth and Planetary Sciences, Faculty of Sciences, Kyushu University

The stratigraphic variation of grain-size distribution (GSD) of pyroclastic fall deposit records the time variation which may reflect the time variation of GSD in the umbrella eruption cloud. In order to relate the stratigraphic variation of GSD and the time variation of umbrella eruption cloud GSD, it is necessary to consider the transportation process of ejecta.

Iriyama and Toramaru (2014, AGU) formulate the mathematical relationship between the depositional structure and the source (the umbrella eruption cloud upward in a vertical direction from the sedimentation point) parameters under the 1D constant height model in which the source height and the source GSD are constant with time throughout a release duration. In this case, we showed that the thickness ratio of the upper and lower layers, which is defined as the ratio of the thickness of the upper layer above the extinction point of the largest grain to whole layers depends on the ratio of the source height, the source GSD, and release duration. In nature, however, the eruption column height or ash cloud height may change even during continuous eruptions such as plinian type. In this study, we numerically assess the influence of the linear increase in the source height on the sorting structure of deposits in the simplest case.

When the linear increase rate in the source height is given as constant b, the increase in b makes the sedimentation duration longer than in the constant height model at the sedimentation surface. The numerical simulations for the linear increase height model are carried out with varying b under the same conditions of the initial source height, the source GSD, and release duration. Results show that the linear increase constant b have a negative correlation with the peak accumulation rate and have a positive correlation with the thickness ratio of the upper layer. These suggest that the increase in the source height (eruption intensity) can be detected from the thickness ratio of the upper layer which can be observed by the geological survey.

Keywords: pyroclastic fall deposits, grain-size distribution, development of eruption

Japan Geoscience Union Meeting 2015
(May 24th - 28th at Makuhari, Chiba, Japan)

SVC46-P17 Room:Convention Hall Time:May 25 18:15-19:30

The Tephra Fall Simulations of the Ignimbrite Eruption of Aso Volcano

ISHII, Kensuke[1*] ; SUZUKI, Yujiro[2] ; SHIMBORI, Toshiki[1] ; FUKUI, Keiichi[1] ; SATO, Eiichi[1]

[1]Meteorological Research Institute, [2]Earthquake Research Institute, The University of Tokyo

For aviation safety, Tokyo Volcanic Ash Advisory Center (Tokyo VAAC) of Japan Meteorological Agency (JMA) operates the tephra prediction system using the Global Atmospheric Transport Model (JMA-GATM) in which JMA Global Forecast or JMA Global Analysis (JMA, 2013) is applied to the atmospheric conditions. JMA-GATM calculates the time evolution of tephra dispersal due to the advection by wind, the diffusion, the gravitational settling, and the wet/dry deposition. Using this model, we have performed the tephra fall simulations for possible ignimbrite eruption (Tatsumi et al, 2014) at Aso volcano in Japan.

The ignimbrite eruptions had been occurred 4 times at the Aso volcano in the past 300,000 years. The Aso-4 ignimbrite eruption (90ka) is considered to be largest among these four eruptions. The tephra particles from this eruption were distributed widely in Japan (Aso-4 tephra); the tephra fall deposits in Hokkaido (1700km far from the volcano) have thickness of about 15cm. In this study, we performed the numerical simulations of tephra fall for the ignimbrite eruption whose intensity is comparable with the Aso-4. In these simulations, it is assumed that the constant emission of the tephra continues for 20 hours, and the total amount of tephra is $7.2*10^{14}$kg.

In JMA operation, an initial distribution of tephra particles for JMA-GATM is given from the estimation using the eruption column model (Suzuki, 1983) or the satellite observation. In the present study, we carried out a numerical simulation of eruption cloud using three-dimensional fluid-dynamics model (Suzuki et al, 2005) in order to estimate an accurate initial distribution of tephra particles. The tracer distribution at 3.5 hours from the initiation of eruption which are obtained from the 3D simulation is used as an initial setting for JMA-GATM. Because JMA-GATM calculates the time evolution of the tephra particles which are advected by wind, the particles with a large velocity difference from the wind are eliminated from initial setting. Using JMA-Global forecast at 12UTC 3 April 2014 as meteorological field, the 3 days tephra forecast starting at 3.5 hours from the initiation of eruption is computed by JMA-GATM. Under this condition, the tephra particles are transported by the mid-tropospheric southwest wind and widely deposited in Japan. The simulation results show the tephra fall deposits of 10 cm in Hokkaido, which is consistent with the geological survey of Aso-4 tephra. In addition, we performed a parametric study of meteorological field with the same initial distribution of tephra. The simulation results indicate that the depositional pattern of fallout largely depends on the meteorological field. In some cases, the most of the tephra particles are settled not on the land in Japan but on the Pacific Ocean.

Keywords: Atmospheric Transport Model, ignimbrite eruption, tephra, tephra fall, numerical simulation

SVC46-P18 Room:Convention Hall Time:May 25 18:15-19:30

Quasi-Realtime Contents of the Tephra Fall Simulations against Large-Scale Eruption

SHIMBORI, Toshiki[1*] ; ISHII, Kensuke[1] ; SATO, Eiichi[1] ; FUKUI, Keiichi[1] ; YOKOYAMA, Hirofumi[1]

[1]Meteorological Research Institute

From FY2014, the Meteorological Research Institute (MRI) of the Japan Meteorological Agency (JMA) is working on research of immediate monitoring and accurate prediction of volcanic phenomena caused by large-scale eruption. Target of the large-scale eruption is the domestic volcano with the volume of ejecta on the order of 10^9 m^3, however, such large-scale eruption has not occurred over the past century. Therefore it is important to simulate the tephra fall against a large-scale eruption in day-to-day weather conditions, from the point of view of roughly predicting the affected area, and also checking and improving the numerical model. For these purposes, assuming the large-scale eruption at Fuji volcano in 1707 (VSJ2013, **P45**) or Sakurajima volcano in 1914 (JpGU2014, **SVC50-P01**), the Volcanology Research Department of the MRI has made the quasi-realtime Internet contents of the large-scale tephra fall predictions with the JMA Regional Atmospheric Transport Model (RATM) driven by the most recent grid point values of the Mesoscale Analysis.

In this presentation, we will introduce the contents planned to daily update on the MRI website.

Keywords: Atmospheric Transport Model, large-scale eruption, volcanic ash, tephra fall, quasi-realtime, numerical simulation

Japan Geoscience Union Meeting 2015
(May 24th - 28th at Makuhari, Chiba, Japan)

SVC46-P19 Room:Convention Hall Time:May 25 18:15-19:30

Numerical assessment of the potential for future limnic eruptions in Cameroon, based on regular monitoring data

KOZONO, Tomofumi[1*] ; KUSAKABE, Minoru[2] ; YOSHIDA, Yutaka[3] ; NTCHANTCHO, Romaric[4] ; OHBA, Takeshi[5] ; TANYILEKE, Gregory[4] ; HELL, Joseph V.[4]

[1]Science, Tohoku Univ., [2]Science, Univ. of Toyama, [3]Yoshida Cons. Eng. Office, [4]IRGM, [5]Science, Tokai Univ.

A limnic eruption is a gas outburst from a lake, and it can cause a catastrophic disaster in the surrounding area. Lakes Nyos and Monoun in Cameroon, Central Africa, are volcanic crater lakes where limnic eruptions with catastrophic releases of CO_2 gas occurred in 1986 (Nyos) and 1984 (Monoun), claiming close to 1800 lives. To understand the mechanism of the limnic eruptions in these lakes, regular monitoring of the chemical composition of the lake water has been conducted since the limnic eruptions, and it allows us to obtain detailed information about CO_2 profiles in the lakes. In this study, we assessed their eruptive potential at Lakes Nyos and Monoun, on the basis of numerical modeling and the CO_2 profiles obtained by the regular monitoring of the lakes.

The evolution of the CO_2 profiles suggests one particular scenario for producing an eruption: supply of CO_2-undersaturated fluid from the lake bottom that induces upwards growth of the bottom layer, leading eventually to CO_2-saturation at mid-depths of the lake. By using a numerical model for the ascent of a plume of CO_2 bubbles, we investigated whether bubble formation in this scenario leads to a bubble plume reaching the lake surface (i.e., a limnic eruption). We found that under realistic conditions (e.g., a CO_2 profile deduced from the regular monitoring data), a bubble plume generated from mid-depths can reach the lake surface with a CO_2 high flux, which corresponds to a limnic eruption. This indicates that the ascent of the bubble plume caused by the upward growth of the CO_2-undersaturated layer is a possible mechanism for inducing a limnic eruption.

Another important factor that affects the current CO_2 profiles in Lakes Nyos and Monoun is the artificial removal of dissolved CO_2 (“controlled degassing”) using degassing pipes. As CO_2-rich water is withdrawn from the deep layer through a pipe, the pipe flow becomes self-sustaining due to bubble formation and expansion caused by decompression in the rising water column. This leads to the formation of a fountain on the lake surface. The most recent CO_2 profiles obtained by the regular monitoring indicate a drastic decrease in the CO_2 concentration at the bottom of the lake. We developed a numerical model for degassing pipe flow so that we could investigate the effects of changes in CO_2 concentration at the lake bottom on the dynamics of the pipe flow and the degree of degassing. From the model, the quantitative relationship between CO_2 concentration at the lake bottom and fountain height observed on the surface of the lake is established. Our results agree well with the observed heights, indicating that our model is successful in capturing the dynamics of the degassing pipe flow in Lakes Nyos and Monoun.

Keywords: Limnic eruption, Lake Nyos, Lake Monoun, Numerical model, Degassing pipe